

Steady State Isotopic Transient Kinetic Analysis of the Ethanol Coupling Reaction
Catalyzed by Magnesia

A Thesis

Presented to
the faculty of the School of Engineering and Applied Science
University of Virginia

in partial fulfillment
of the requirements for the degree

Master of Science

by

Theodore W. Birky

August

2012

APPROVAL SHEET

The thesis
is submitted in partial fulfillment of the requirements
for the degree of
Master of Science

Theodore W. Birky
AUTHOR

The thesis has been read and approved by the examining committee:

Robert J. Davis
Advisor
David R. L.
Don H. L.

Accepted for the School of Engineering and Applied Science:

James H. Ayl

Dean, School of Engineering and Applied Science

August
2012

Abstract

Although ethanol can be produced on a large scale by fermentation, its use as a transportation fuel has several drawbacks. Ethanol can be coupled to form butanol, a more desirable fuel, over basic catalysts via the Guerbet reaction. In this work, the coupling of ethanol to butanol over a magnesia catalyst at 673 K and 1.29 atm has been studied in a fixed bed reactor using an isotopic transient method.

The transient method enabled surface coverages and the intrinsic rate of the catalytic cycle to be measured. At 673 K, the fractional coverage of absorbed ethanol under steady state reaction conditions was 0.51 relative to the number of exposed MgO atom pairs on the surface, whereas the coverage of surface intermediates was less than 0.1, depending on the conversion in the reactor. The intrinsic rate at which the catalytic cycle turned over was found to be 0.04 s^{-1} at 673 K. These results suggest that only a small fraction of the MgO surface is involved in the coupling reaction, presumably through aldol condensation reactions, and that adsorbed ethanol present on the surface prevents multiple condensation events from deactivating the catalyst.

Acknowledgements

I would like to thank my advisor, Robert Davis, for his assistance in all my work throughout this experience at the University of Virginia. I would also like to thank the current and past members of the Davis lab that have helped me numerous times: Bhushan Zope, Joseph Kozlowski, Sara Davis, Matthew Ide, Heng Shou, Derek Falcone, Juan Lopez-Ruiz, Sabra Hanspal, Benjamin Huang, and Kehua Yin. Acknowledgements also go out to the staff of the Chemical Engineering Department: Ricky Buchanan, Vickie Faulconer, Teresa Morris, and Kim Doerr. This work was supported by a grant from the Department of Energy, Basic Energy Sciences (DE-FG02-95ER14549).

Table of Contents

Title Page	
Approval Sheet	
Abstract	1
Acknowledgements	2
List of Figures	4
List of Symbols	8
Chapter 1: Introduction	9
Chapter 2: Background of the Guerbet Reaction	11
Chapter 3: Steady State Isotopic Transient Kinetic Analysis (SSITKA)	16
Chapter 4: Experimental Methods	21
Chapter 5: Results and Discussion	29
Chapter 6: Conclusions	44
Appendix	46
References	53

List of Figures

Figure 1: Billions of gallons of ethanol produced in the United States each year.

Figure 2: Example of isotopic transient. The concentrations are normalized.

Figure 3: Schematic of the system used

Figure 4: NIST Cracking Pattern of Ethanol.

Figure 5: NIST Cracking Pattern of Acetaldehyde

Figure 6: NIST Cracking Pattern of Butanol

Figure 7: Mass spectrum of product stream from the ethanol coupling reaction over MgO

Figure 8: Relationship between the observed conversion of ethanol as a function of inverse total flow rate

Figure 9: Isotopic transient curve for unlabeled butanol ($m/z=56$) after switching from unlabeled ethanol to ^{13}C labeled ethanol with a total flow rate of $25\text{ cm}^3\text{ min}^{-1}$ during a reaction at 3.5 mmol L^{-1} ethanol, 0.2 g of MgO, 673 K, and 1.3 atm

Figure 10: Isotopic transient curve for unlabeled butanol ($m/z=56$) after switching from unlabeled ethanol to ^{13}C labeled ethanol with a total flow rate of $50\text{ cm}^3\text{ min}^{-1}$ during a reaction at 3.5 mmol L^{-1} ethanol, 0.2 g of MgO, 673 K, and 1.3 atm

Figure 11: Isotopic transient curve for unlabeled butanol ($m/z=56$) after switching from unlabeled ethanol to ^{13}C labeled ethanol with a total flow rate of $75\text{ cm}^3\text{ min}^{-1}$ during a reaction at 3.5 mmol L^{-1} ethanol, 0.2 g of MgO, 673 K, and 1.3 atm

Figure 12: Isotopic transient curve for unlabeled butanol ($m/z=56$) after switching from unlabeled ethanol to ^{13}C labeled ethanol with varying total flow rates during a reaction at 3.5 mmol L^{-1} ethanol, 0.2 g of MgO , 673 K, and 1.3 atm

Figure 13: Relationship between the observed characteristic tau of butanol as a function of inverse total flow rate

Figure 14: Isotopic transient curve for unlabeled ethanol ($m/z=31$) after switching from unlabeled ethanol to ^{13}C labeled ethanol with a total flow rate of $25 \text{ cm}^3 \text{ min}^{-1}$ during a reaction at 3.5 mmol L^{-1} ethanol, 0.2 g of MgO , 673 K, and 1.3 atm

Figure 15: Isotopic transient curve for unlabeled ethanol ($m/z=31$) after switching from unlabeled ethanol to ^{13}C labeled ethanol with a total flow rate of $50 \text{ cm}^3 \text{ min}^{-1}$ during a reaction at 3.5 mmol L^{-1} ethanol, 0.2 g of MgO , 673 K, and 1.3 atm

Figure 16: Isotopic transient curve for unlabeled ethanol ($m/z=31$) after switching from unlabeled ethanol to ^{13}C labeled ethanol with a total flow rate of $75 \text{ cm}^3 \text{ min}^{-1}$ during a reaction at 3.5 mmol L^{-1} ethanol, 0.2 g of MgO , 673 K, and 1.3 atm

Figure 17: Effect of Flow Rate on Characteristic tau for Ethanol

Figure 18: Relationship between the rate of butanol production as a function of the acetaldehyde concentration at the exit of the reactor.

Figure 19: Comparing the Effect of Flow Rate on the Characteristic tau for Ethanol and Butanol

Figure 20: Analysis of ethanol in an empty reactor switch at 25 mL min^{-1}

Figure 21: Analysis of ethanol in an empty reactor switch at 50 mL min^{-1}

Figure 22: Analysis of ethanol in an empty reactor switch at 75 mL min^{-1}

Figure 23: Effect of flow rate on space time of ethanol.

Figure 24: Isotopic transient curve for unlabeled butanol ($m/z=56$) after switching from unlabeled ethanol to ^{13}C labeled ethanol with a total flow rate of $25\text{ cm}^3\text{ min}^{-1}$ during a reaction at 3.5 mmol L^{-1} ethanol, 0.2 g of MgO , 673 K , and 1.3 atm . Raw data.

Figure 25: Isotopic transient curve for unlabeled butanol ($m/z=56$) after switching from ^{13}C labeled ethanol to unlabeled ethanol with a total flow rate of $25\text{ cm}^3\text{ min}^{-1}$ during a reaction at 3.5 mmol L^{-1} ethanol, 0.2 g of MgO , 673 K , and 1.3 atm . Raw data.

Figure 26: Isotopic transient curve for unlabeled butanol ($m/z=56$) after switching from unlabeled ethanol to ^{13}C labeled ethanol with a total flow rate of $50\text{ cm}^3\text{ min}^{-1}$ during a reaction at 3.5 mmol L^{-1} ethanol, 0.2 g of MgO , 673 K , and 1.3 atm . Raw data.

Figure 27: Isotopic transient curve for unlabeled butanol ($m/z=56$) after switching from ^{13}C labeled ethanol to unlabeled ethanol with a total flow rate of $50\text{ cm}^3\text{ min}^{-1}$ during a reaction at 3.5 mmol L^{-1} ethanol, 0.2 g of MgO , 673 K , and 1.3 atm . Raw data.

Figure 28: Isotopic transient curve for unlabeled butanol ($m/z=56$) after switching from unlabeled ethanol to ^{13}C labeled ethanol with a total flow rate of $75\text{ cm}^3\text{ min}^{-1}$ during a reaction at 3.5 mmol L^{-1} ethanol, 0.2 g of MgO , 673 K , and 1.3 atm . Raw data.

Figure 29: Isotopic transient curve for unlabeled butanol ($m/z=56$) after switching from ^{13}C labeled ethanol to unlabeled ethanol with a total flow rate of $75\text{ cm}^3\text{ min}^{-1}$ during a reaction at 3.5 mmol L^{-1} ethanol, 0.2 g of MgO , 673 K , and 1.3 atm . Raw data.

Figure 30: Isotopic transient curve for unlabeled butanol ($m/z=56$), ^{12}C - ^{13}C -butanol ($m/z=58$), and ^{13}C -butanol ($m/z=60$) after switching from unlabeled ethanol to ^{13}C

labeled ethanol with a total flow rate of $25 \text{ cm}^3 \text{ min}^{-1}$ during a reaction at 3.5 mmol L^{-1} ethanol, 0.2 g of MgO, 673 K, and 1.3 atm. Raw data.

Figure 31: Isotopic transient curve for unlabeled butanol ($m/z=56$), ^{12}C - ^{13}C -butanol ($m/z=58$), and ^{13}C -butanol ($m/z=60$) after switching from ^{13}C labeled ethanol to unlabeled ethanol with a total flow rate of $25 \text{ cm}^3 \text{ min}^{-1}$ during a reaction at 3.5 mmol L^{-1} ethanol, 0.2 g of MgO, 673 K, and 1.3 atm. Raw data.

Figure 32: Isotopic transient curve for unlabeled butanol ($m/z=56$), ^{12}C - ^{13}C -butanol ($m/z=58$), and ^{13}C -butanol ($m/z=60$) after switching from unlabeled ethanol to ^{13}C labeled ethanol with a total flow rate of $50 \text{ cm}^3 \text{ min}^{-1}$ during a reaction at 3.5 mmol L^{-1} ethanol, 0.2 g of MgO, 673 K, and 1.3 atm. Raw data.

Figure 33: Isotopic transient curve for unlabeled butanol ($m/z=56$), ^{12}C - ^{13}C -butanol ($m/z=58$), and ^{13}C -butanol ($m/z=60$) after switching from ^{13}C labeled ethanol to unlabeled ethanol with a total flow rate of $50 \text{ cm}^3 \text{ min}^{-1}$ during a reaction at 3.5 mmol L^{-1} ethanol, 0.2 g of MgO, 673 K, and 1.3 atm. Raw data.

Figure 34: Isotopic transient curve for unlabeled butanol ($m/z=56$), ^{12}C - ^{13}C -butanol ($m/z=58$), and ^{13}C -butanol ($m/z=60$) after switching from unlabeled ethanol to ^{13}C labeled ethanol with a total flow rate of $75 \text{ cm}^3 \text{ min}^{-1}$ during a reaction at 3.5 mmol L^{-1} ethanol, 0.2 g of MgO, 673 K, and 1.3 atm. Raw data.

Figure 35: Isotopic transient curve for unlabeled butanol ($m/z=56$), ^{12}C - ^{13}C -butanol ($m/z=58$), and ^{13}C -butanol ($m/z=60$) after switching from ^{13}C labeled ethanol to unlabeled ethanol with a total flow rate of $75 \text{ cm}^3 \text{ min}^{-1}$ during a reaction at 3.5 mmol L^{-1} ethanol, 0.2 g of MgO, 673 K, and 1.3 atm. Raw data.

List of Symbols

Symbol	Name	Units
θ	Fractional coverage of the catalyst	$\text{mol}_{\text{prod}} \text{mol}_{\text{surface cat}}^{-1}$
k	First order rate constant	s^{-1}
t	Time	s
τ	Mean surface residence time	s
T.o.F.	Turn over frequency	s^{-1}
\bar{C}	Relative Concentration	-
R	Rate of production	$\text{mol m}^{-2} \text{s}^{-1}$
F	Flow rate	$\text{cm}^3 \text{min}^{-1}$
N	Surface coverage of intermediates	mol m^{-2}

Steady State Isotopic Transient Kinetic Analysis of the Ethanol Coupling Reaction Catalyzed by Magnesia

Chapter 1: Introduction

Butanol is currently an important chemical used in industry, because it is used to produce butyl esters, butyl ethers, pharmaceuticals, and various plastics. It is also used commercially in certain dyes, lacquers, resins, films, rubber cement, etc. [1]

When comparing butanol to ethanol in terms of a transportation fuel, butanol is the better choice. For example, the energy value of butanol (110,000 BTU/Gal) is greater than that of ethanol (76,100BTU/Gal) and is much closer to that of gasoline (114,800 BTU/Gal). Butanol is non-corrosive and less hydrophilic and therefore can be shipped by pipeline instead of being transported by trucks. [2]

Producing butanol efficiently is a challenge that people are still trying to solve. One important way to synthesize butanol is to combine propylene with hydrogen and carbon monoxide via hydroformylation to prepare butyraldehyde, which can be subsequently hydrogenated into butanol. The hydroformylation step in the process is not completely selective as it creates both butyraldehyde (linear) and isobutyraldehyde (branched), and it requires an expensive rhodium-based catalyst to proceed. [1]

Butanol can also be synthesized from ethanol. Ethanol is produced in numerous ways, most commonly by fermentation of sugars. [3] The production of ethanol is a rapidly growing industry and can be a great feed source for the production of butanol, as shown in figure 1. In 2011, 13.9 billion gallons of ethanol were produced in the United States. [4]

Ethanol Production in the U.S

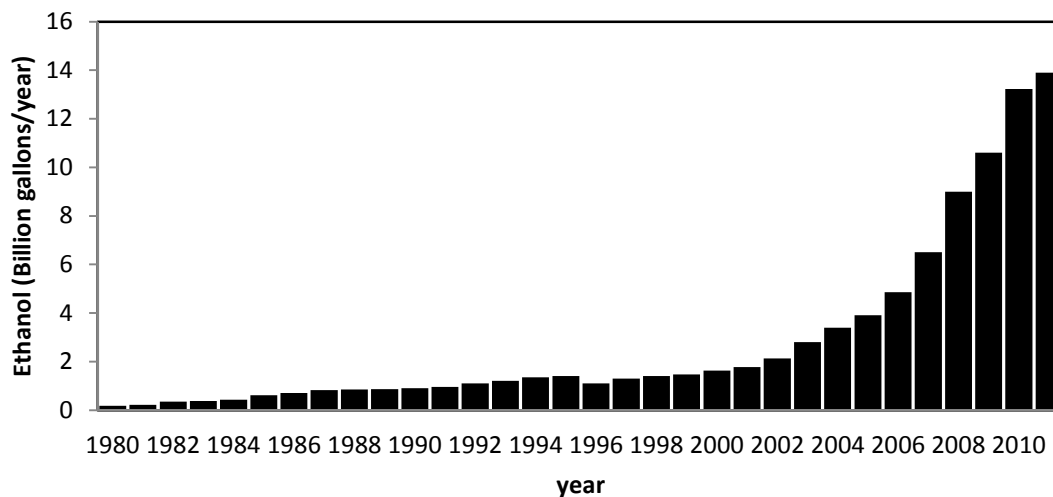


Figure 1: Billions of gallons of ethanol produced in the United States each year. [4]

The focus of this thesis research is the conversion of the two ethanol molecules to produce a butanol molecule over a solid base catalyst. This general reaction class of alcohol coupling is known as the Guerbet reaction. To study this reaction, the technique of steady-state isotopic transient kinetic analysis was used.

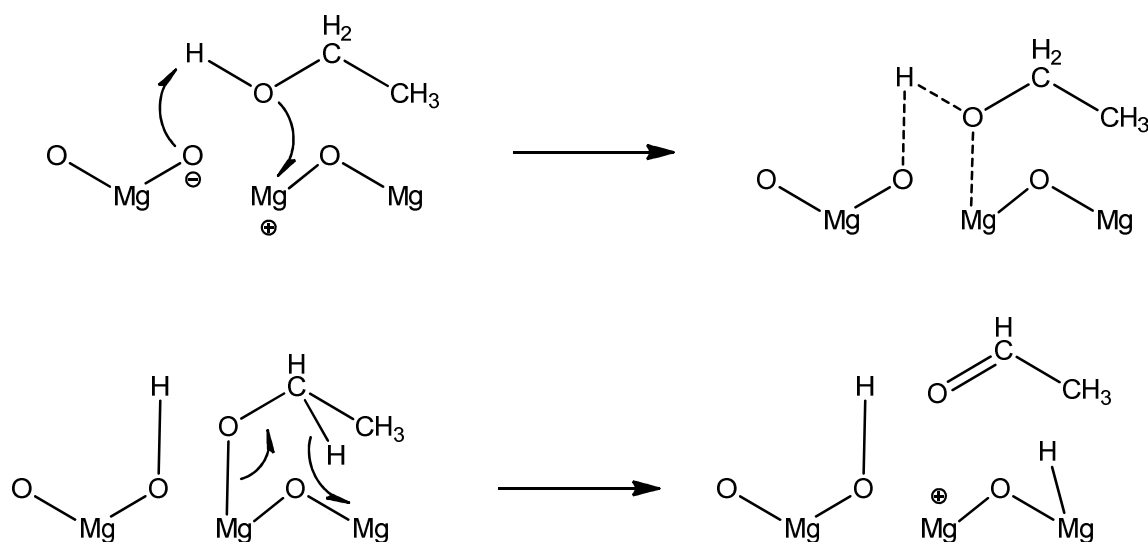
Chapter 2: Background of the Guerbet Reaction

The Guerbet reaction is an organic reaction with the assistance of a catalyst to combine two alcohol molecules into one with the loss of a water molecule. This process was observed in the 1890's by a chemist named Marcel Guerbet. The Guerbet reaction is useful for creating long chain alcohols with high-purity branching. [5] This reaction is used in industry to create molecules for many applications such as metal lubrication, plastic mold release, paper processing, synlube, and personal care products. [6]

Although the Guerbet reaction has been studied for many years, the mechanism for the reaction is still debated. S. Veibel and J. I. Neuen have proposed the following mechanism for the reaction. The steps illustrated below occur on a magnesia (MgO) surface as a catalyst.

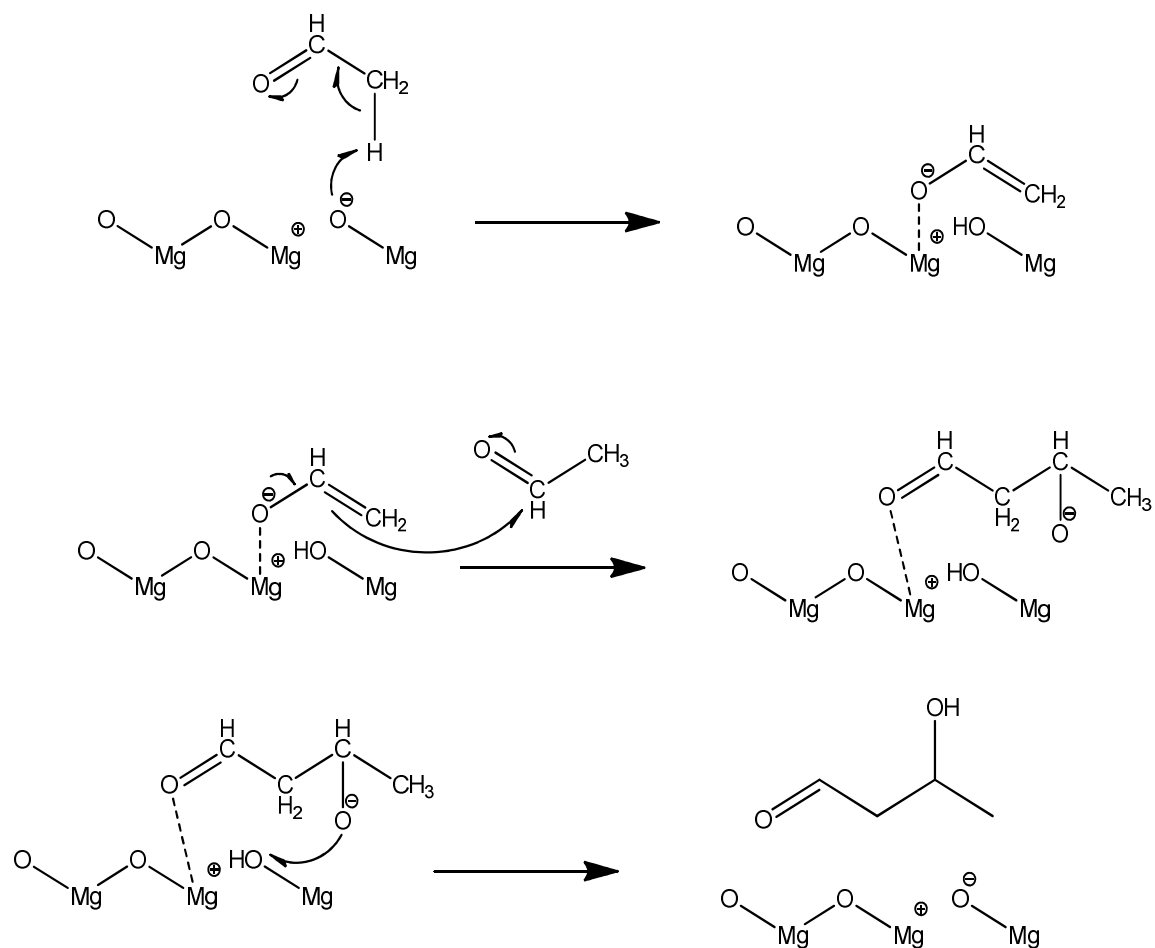
First, ethanol is dehydrogenated into an aldehyde. [7]

(Step 1)



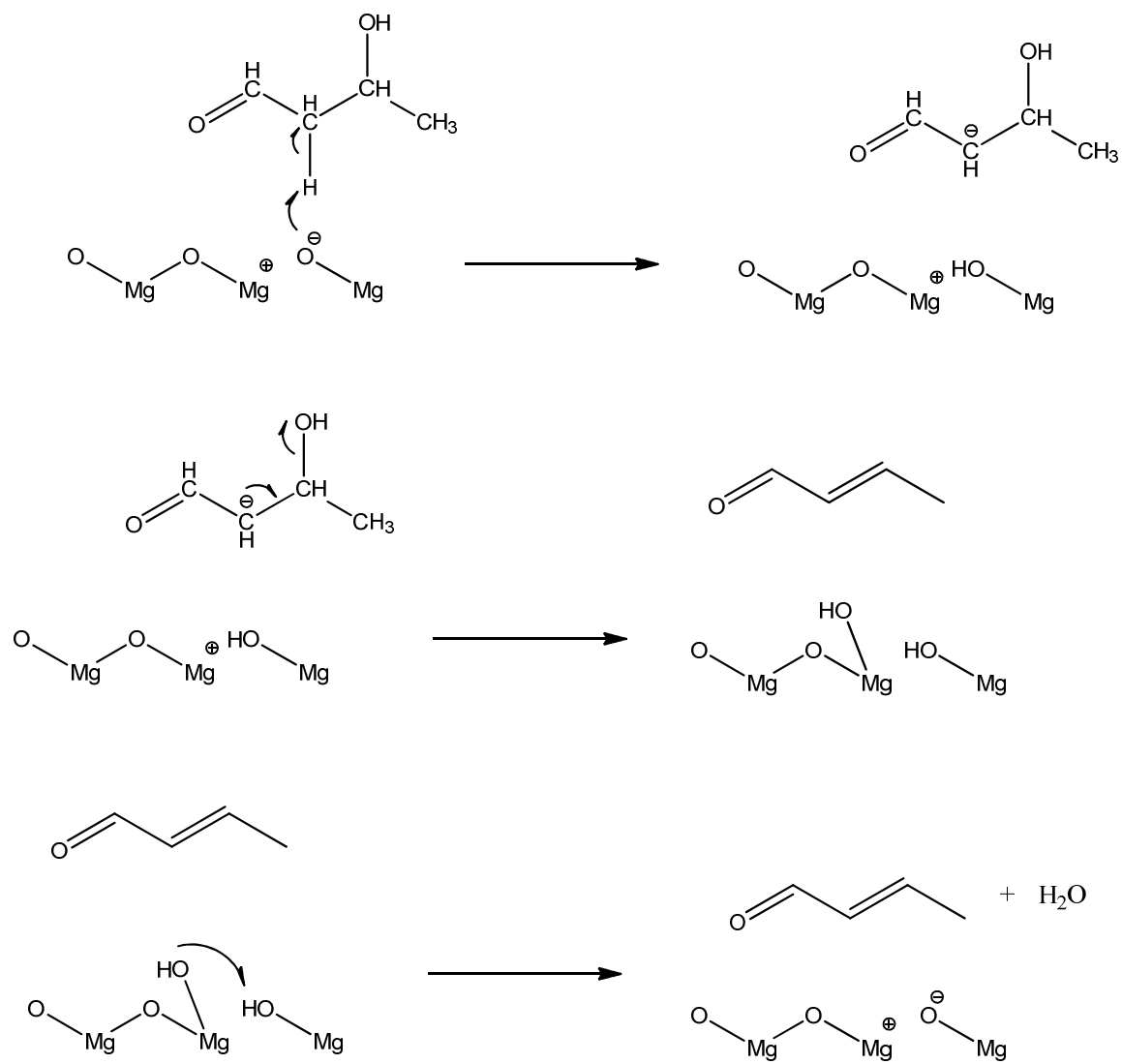
Second, the aldehyde combines with another aldehyde through an aldol condensation reaction sequence. [7]

(Step 2)



After the coupling of aldehydes, the aldol intermediate proceeds through a dehydration reaction. [7]

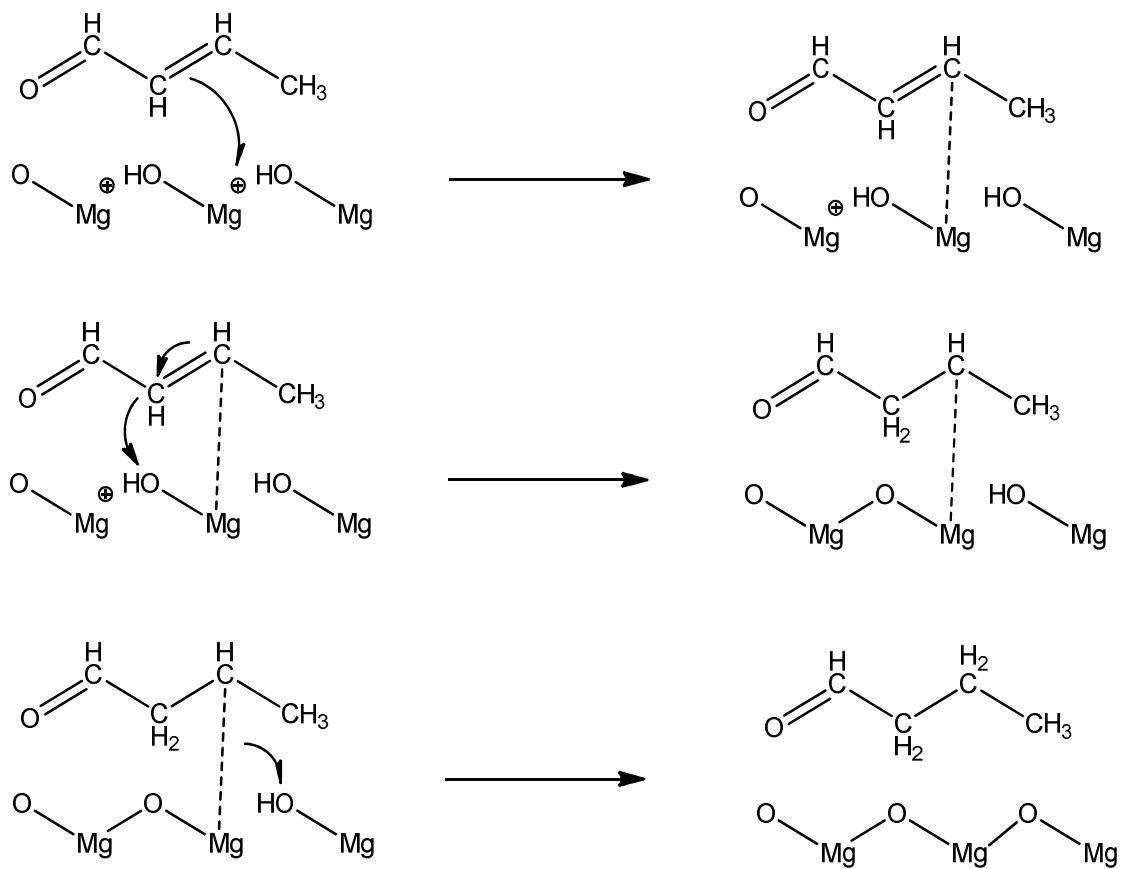
(Step 3)



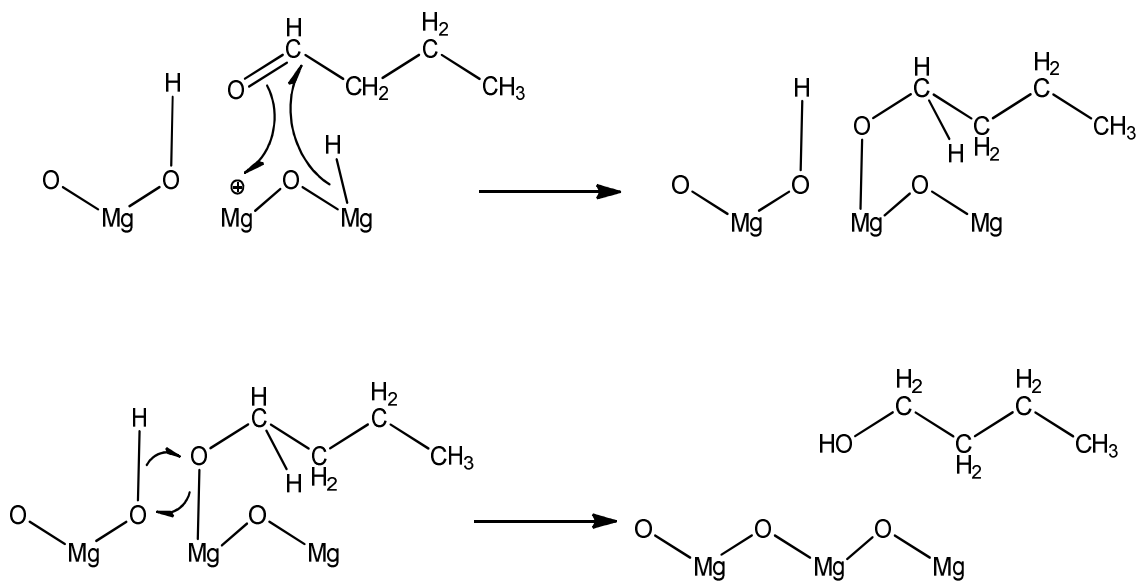
Finally the allylic aldehyde is sequentially hydrogenated by the catalyst to form butanol.

[7]

(Step 4)



(Step 5)



Although ethanol coupling to butanol produces a linear alcohol, Guerbet coupling of higher alcohols gives branched products. Guerbet alcohols are useful for many applications because of their branching and high molecular weight. The alcohols have low irritation potential, extremely low freezing temperatures, low volatility, and are used to make many derivatives, as super fatting agents, and are good lubricants. [6]

In a study done by Matsu-Ura, Toyomi et al., numerous Guerbet alcohols are achieved through reactions using different iridium complex catalysts. [8] C. Carlini has done numerous studies on the Guerbet reaction. In a three part series, "Selective synthesis of isobutanol by means of the Guerbet reaction," using methanol and n-propanol, he studied numerous catalysts and catalyst compositions, various temperatures, types of gas in the surrounding atmosphere, and pressures to study the reaction. [9][10][11] In the study "Guerbet condensation of methanol with n-propanol to isobutyl alcohol over heterogeneous bifunctional catalysts based on Mg–Al mixed oxides partially substituted by different metal components," metal oxides were used as catalysts and had higher activity and selectivity than the copper chromite that was used previously. [12] Although many studies of the Guerbet reaction have been performed, fundamental kinetic parameters associated with the reaction are lacking. Therefore, a goal of this thesis is to measure some of the critical kinetic parameters for ethanol coupling over a well-known solid base, MgO.

Chapter 3: Steady State Isotopic Transient Kinetic Analysis (SSITKA)

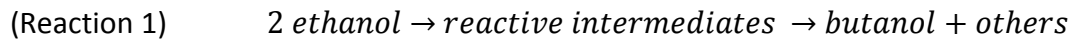
Catalysts are materials that are used in a process to change the rate of a chemical reaction, but are never consumed by the reaction. When a catalyst is present in a reaction, the reaction rate is based on some property of the catalyst, typically the mass. This is done to help determine the effectiveness of the catalyst being used. When a catalyst is a solid, however, that basis can be misleading. A solid catalyst can only affect the reaction at the surface of the solid. To correct for this difference, the reaction rate is based on the surface area of the catalyst. This can be measured by physical adsorption of gases. This method determines the exposed surface of the material, but cannot determine how much of the exposed surface is actively participating in the reaction.

Chemisorption of an active adsorbate can provide an estimate of the number of active sites on a surface, but even this method is an approximation. A turn-over-frequency (TOF (molecules reacting per active site in a unit of time)) can be determined from the number of active adsorbed surface intermediates that participate in a catalytic cycle. This technique is called Steady State Isotopic Transient Kinetic Analysis (SSITKA).

SSITKA studies the transient behavior of the products of a known reaction occurring on a catalyst by means of a rapid analysis of the gas phase after a change in reactant. This step change during a steady-state reaction is accomplished by using isotopically-labeled reactants so that the steady state is not perturbed. This method is useful because only the reactive intermediates on the catalyst that lead to products are characterized and all the spectator species can be neglected on the catalyst. Most other

methods for characterizing sites on catalysts would count both active and non-active sites on the surface.

The theory behind isotopic transient analysis is simple, but needs an explanation. What follows was first presented by Biloen [13] and Shannon and Goodwin. [14] First, the following reaction will be considered.



A first order rate constant, k , will be defined as the reciprocal value of the average lifetime of the reactive intermediates on the catalyst surface. The value of k can be obtained from steady-state kinetics, since the rate of product formation is the product of k and the concentration of the reactive intermediates on the surface.

(Equation 1) $\text{rate of production of butanol} = k * \theta_{RI}$

To solve for k , the concentration of the reactive intermediates on the surface must be known. If a mass balance is done on the reactive intermediates at steady state when there is no accumulation, the mass balance becomes:

(Equation 2)

$$d\theta_{RI}/dt = \text{rate of production of reactive intermediates}$$

$$- \text{rate of production of butanol} = 0$$

If the feed of ethanol to the system was instantaneously stopped, equation 2 would become:

(Equation 3) $d\theta_{RI}/dt = -\text{rate of production of butanol}$

If equation 1 is substituted into equation 3, and integration is done, with time=0 being when the feed of A is stopped, the equation becomes:

(Equation 4)
$$\theta_{RI_t} = \theta_{RI_{t=0}} * e^{(-k*t)}$$

Substituting equation 4 into equation 1 produces:

(Equation 5)
$$d[butanol]/dt = k * \theta_{RI_{t=0}} * e^{(-k*t)}$$

From this approach, the concentration of the reactive intermediates can be found from the concentration of butanol. This derivation assumes that k is independent of the concentration of ethanol, which is not always true. An example of this situation is the reaction of CO and H₂ to form CH₄ over transition metals. [15] The adsorption of CO on the metal surface is stronger than the adsorption of H₂ on the metal surface. This means, that when CO is no longer fed to the reactor, a significant rise in the H₂ surface coverage is observed, which has an impact on the conversion of CO to CH₄. This means that the steady state kinetics is not maintained. To keep the steady state kinetics in this situation, the reactant that is being removed from the system needs to be replaced with an isotopically-labeled equivalent. In this example for CO and H₂, ¹²CO is no longer fed to the system and therefore needs to be replaced. A suitable candidate for a replacement would be ¹³CO. [13]

It is easier to obtain the value of k through transient techniques. One can solve for the rate constant, k, by measuring the mean surface residence time of the reactive intermediates, τ . The mean surface residence time is based on how long the intermediates reside on the surface of the catalyst throughout a catalytic cycle. To

calculate this value, an integration of the figure below is required. The figure shows a switch of the reactant from normal (^{12}C) ethanol to ^{13}C -labelled ethanol. This allows the transient to occur without disturbing the steady state conditions, and enables the product to be followed with a mass spectrometer.

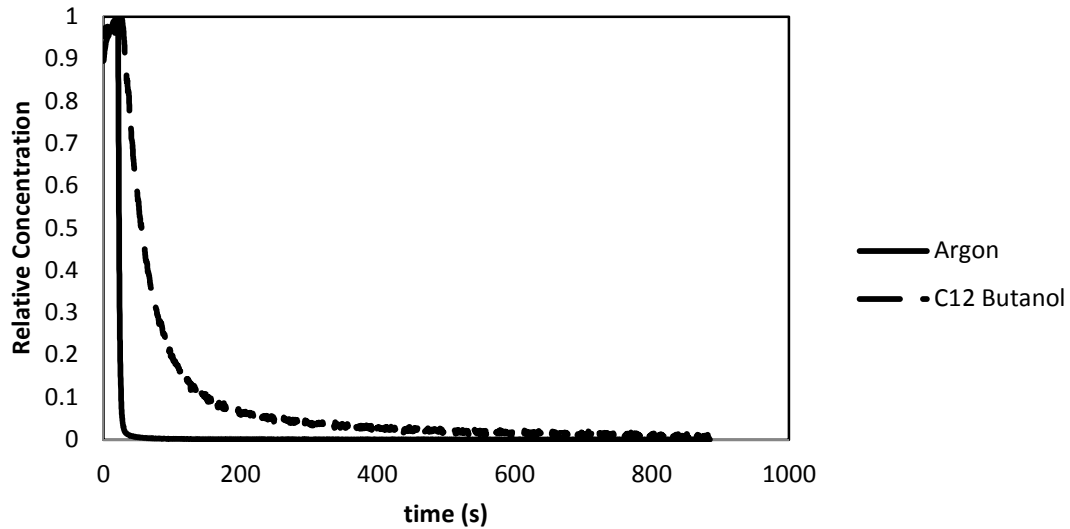


Figure 2: Example of isotopic transient. The concentrations are normalized.

The integral that needs to be solved is:

$$\text{(Equation 6)} \quad \tau_{butanol} = \int_0^{\infty} (\bar{C}_{C^{12}butanol} - \bar{C}_{Ar}) dt$$

This value of τ can be used to calculate the intrinsic turnover frequency. The rate constant and the intrinsic turnover frequency are related to the mean surface residence time by the equation:

$$\text{(Equation 7)} \quad T.O.F. = k = 1/\tau_{butanol}$$

Since the mean surface residence time is calculated from the transient response of the product, the observed value can include contributions from readsorption of the

product back onto the surface of the catalyst. [14] This occurrence can lead to a higher value of the mean surface residence time. To account for this, the flow of the feed stream is varied, and the effect on the mean surface residence time is observed. If the mean surface residence time changes with flow rate, the extent of readesorption on τ is observed. With a higher flow rate, there should be a decrease in the likelihood of product molecules readsorbing onto the catalyst surface so the measured mean surface residence time should approach true residence time on the surface.

Steady state isotopic transient kinetic analysis is an underused technique in research. It can help reveal important characteristics of the catalyst in the system. [15] Other studies can use SSITKA to try to understand the reaction mechanism of a given system. [16] [17] [18]

The specific goals of this study are the following: calculate the reaction rate of ethanol coupling over MgO, measure the mean surface residence time of the reaction intermediates, and measure the fractional coverage of reaction intermediates that lead to butanol.

Chapter 4: Experimental Methods

The reaction system is composed of a packed-bed reactor, a four port switching valve, and a mass spectrometer. The unique part of this system is the four port switching valve. It allows the system to switch the feed to the reactor from one line to another almost instantaneously. While feeding carbon-12 ethanol in one line, the system can immediately switch to a carbon-13 ethanol feed while the changes of the products in the reactant stream are monitored by the mass spectrometer. This allows the system to keep the steady-state properties of the reaction while seeing how the system responds to a change of the feed. The 4-port valve is actuated by air pressure. A schematic of the system can be seen in figure 3.

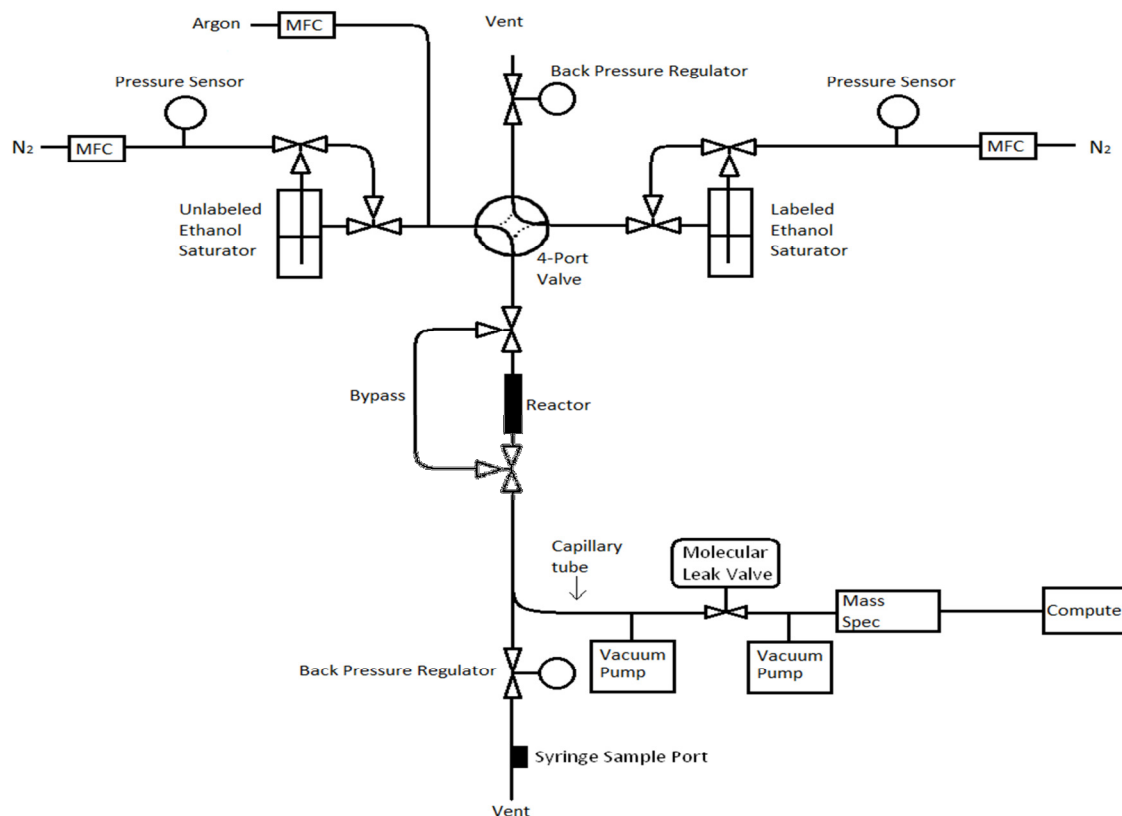


Figure 3: Schematic of the system used

Initially, dinitrogen and argon gas are fed into the system each using a Brooks 5850E mass flow controller. The dinitrogen gas, N_2 , is purified by passage through a Supelco OMI-2 purifier. Using a bubble flow meter and a stopwatch, the mass flow controllers were all calibrated. The flow rates versus controller setting were fit using a linear regression, forcing a fit through the origin. The resulting equation was used to determine the volumetric flow rate at a given controller setting. The calibration was done at room temperature and pressure. The results of the calibration can be seen in Table 1

Table 1: Linear Regression Results to Calculate Flow Rate from Controller Setting

Mass Flow Controller	Gas	Volumetric Flow Rate Slope [mL min^{-1}]	Molar Flow Rate Slope [mol min^{-1}]
1	N_2	3.19	0.0715
4	N_2	2.47	0.0553
8	Ar	0.12	0.00258

Both the labeled ethanol and the unlabeled ethanol were introduced to the system via saturators, or bubblers. The dinitrogen gas, N_2 , is bubbled through the liquid ethanol. The openings in the fritted glass were reported to be between 70-100 μm by Ace Glass Inc. Cambridge Isotopes provided the ^{13}C ethanol. It contained 58,900 ppm of water, which needed to be removed before the reaction could be run so as to not interfere with the steady state conditions. Sigma-Aldrich 3Å molecular sieves were used to dehydrate the ^{13}C ethanol. The sieves were heated to 523 K for 3 h in flowing dinitrogen gas. Once the sieves were dehydrated, they were placed in the bubbler along with the ^{13}C ethanol. The molecular sieves were also put into the unlabeled ethanol in

order to treat both bubblers the same. Sigma-Aldrich provided the unlabeled anhydrous ^{12}C ethanol, which was reported to be 99.5% pure. The saturation pressure was calculated from Antoine's equation. The desire was to obtain a feed with 7.4% ethanol at a total pressure of 20 psia (1.36 atm) to match on-going work by another student in the lab. The desired partial pressure of ethanol was therefore 0.09 atm. The actual partial pressure achieved was 0.080 atm, based on a water bath temperature of 299 K. Following Antoine's equation, the desired temperature of the ethanol-saturated dinitrogen should be approximately 301K. The bubblers were thus heated in a thermostated (PID) water bath.

An inert tracer was also fed to the system to monitor the gas phase hold-up of the reactor. The tracer used in this work was the noble gas argon. The tracer was used to measure the contributions from various time delays, back-mixing, and gas-phase hold-up within the reactor.

The catalyst being tested was the base catalyst magnesium oxide and was selected for a number of reasons. Magnesia, or MgO , is a solid base, well known for catalyzing aldol condensation reactions. [19][20] [21] In a study done by A.S. Ndou, N. Plint, and N.J. Coville, MgO had the highest yield by far of butanol from ethanol when testing eight different catalysts. [22] In a study done by the Research Laboratory of Resources Utilization in Tokyo, it was found that the Guerbet reaction would proceed at atmospheric pressure and elevated temperatures with the catalyst MgO . [23] If an acid catalyst was used, most likely the first step within the mechanism for the Guerbet

reaction shown above would be dehydration instead of a dehydrogenation creating ethene instead of acetaldehyde. [24]

The MgO used in this study was obtained from UBE Industries, LTD. The particle size is approximately $0.048\mu\text{m}$ (480A). The specific surface area is reported to be $34.9\text{ m}^2\text{ g}^{-1}$.

The reactor for this system was operated as differential packed-bed reactor. Each catalyst sample was pressed under four metric tons, then crushed and sieved between 106 and $180\mu\text{m}$. A 200-mg sample of MgO was loaded into a stainless-steel tube using quartz wool to hold the sample in place. The sample was heated at 10 K min^{-1} to 773 K in 50 mL min^{-1} of flowing dinitrogen gas and held at 773K for 1 h. The sample was then cooled to the reaction temperature, 673 K, to measure the reaction kinetics. Steady-state transient responses were collected at total pressure of 1.29 atm and a partial pressure of ethanol of 0.080 atm. The total flow rate varied from 25 mL min^{-1} to 75 mL min^{-1} to examine the effect of readsorption on the catalyst particles.

The isotopic transient responses were acquired by switching between different feed streams of unlabeled and isotopically-labeled ethanol. The switch was controlled by a Valco Instruments Company Inc. 4-port switching valve. To maintain a smooth transition during a switch, back-pressure regulators maintained the lines at approximately the same pressure.

After the reactor, a small amount of product flowed through a side-stream to the mass spectrometer. Using a Balzers-Pfeiffer Prisma 200-amu mass spectrometer, the

concentrations of ^{12}C -ethanol, ^{13}C -ethanol, argon, ^{12}C -butanol, ^{12}C - ^{13}C -butanol, and ^{13}C -butanol ($m/e=31, 32, 40, 56, 58$, and 60 respectively) were monitored continuously.

These values were chosen based on the NIST database cracking pattern as seen below.

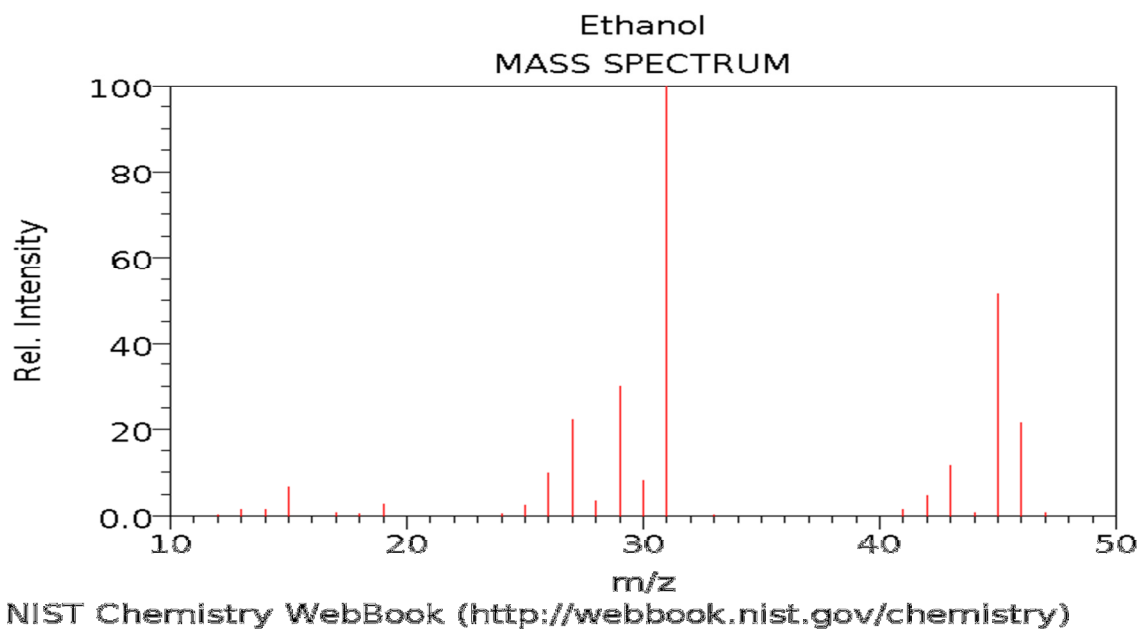


Figure 4: NIST Cracking Pattern of Ethanol. [25]

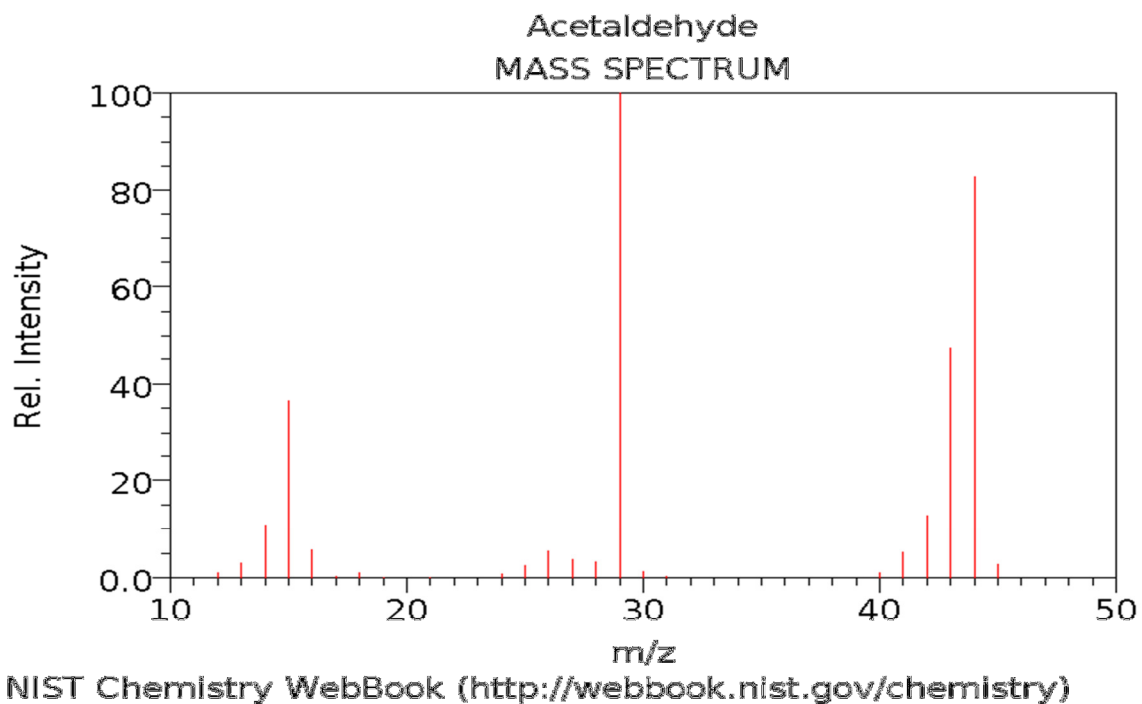


Figure 5: NIST Cracking Pattern of Acetaldehyde [25]

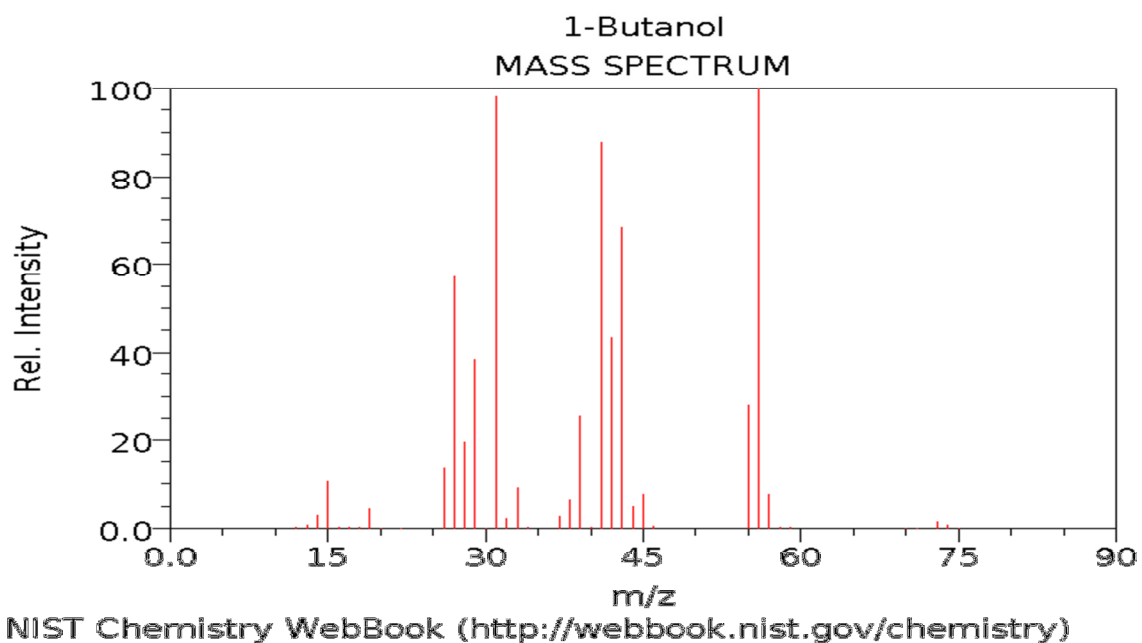


Figure 6: NIST Cracking Pattern of Butanol [25]

The major peaks for ethanol are 45 and 31. Acetaldehyde has peaks at 29 and 44, which are both covered by other signals. The peak at 29 is covered by the large peak

at 28 from dinitrogen and the peak at 44 is covered up from the 45 peak from ethanol. Butanol has its major peaks at 31, 41, and 56. The concentration for butanol should be orders of magnitude smaller than that of ethanol and therefore should not contribute to the signal strength at 31. That allows for the signal at 31 to be scanned for ethanol, acetaldehyde can not be scanned in the mass spectrometer, and the butanol can be scanned at 56. For the ^{13}C labeled ethanol and the ^{13}C labeled butanol, it must be determined how the labeled C will affect the cracking pattern. If ethanol is scanned at 31, it has lost a CH_3 and therefore has CH_2OH remaining which has only 1 carbon atom. That leads to having 32 being the mass that should be scanned for ^{13}C ethanol. For butanol to be scanned at 56, a water molecule has been removed and therefore has C_4H_8 remaining which has 4 carbon atoms. That leads to having 60 being the mass that should be scanned for ^{13}C butanol.

A scan from the mass spectrometer during an ethanol coupling reaction shows some of the major peaks in Figure 4. The major peaks of 31 and 56 can be seen for ^{12}C -ethanol and ^{12}C -butanol respectively. The peak at 28 is the inert carrier gas dinitrogen, N_2 . A large peak is present at $m/e=45$, the contributions at this peak are from ethanol, acetaldehyde, and butanol and therefore the peak is neglected.

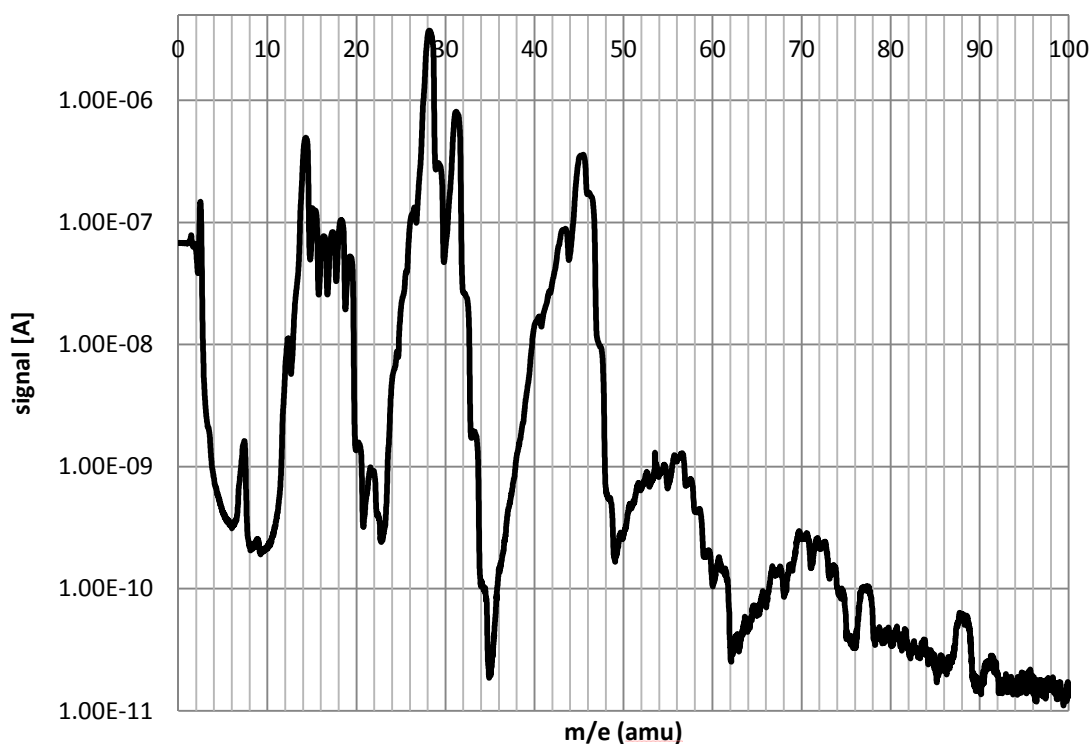


Figure 7: Mass spectrum of product stream from the ethanol coupling reaction over MgO

The butanol signal was calibrated against both the ethanol and the argon signal to determine the amount of butanol produced in the reaction. In addition, a syringe port was installed after the back-pressure regulators so a sample of product could be collected and analyzed in a gas chromatograph. The GC made it possible to observe other known products of the reaction such as ethene and acetaldehyde.

The mass-spectrometer in this system is a quadrupole mass spectrometer, which means that it has four rod electrodes arranged in parallel that form the quadrupole field. A static electrical field accelerates the ions before they fly through the quadrupole field. The quadrupole field between the rods allows only one particle of a given mass to pass through at a time. [26]

Chapter 5: Results and Discussion

The results of the steady-state reaction of 3.5 mmol L⁻¹ ethanol in N₂ over an MgO catalyst (0.2 g) at 673 K and 1.3 atm can be seen in Table 2 and Table 3.

Table 2: Rate of Ethanol Coupling over MgO^a

Total Flow Rate [mL min ⁻¹]	Rate of Production of Butanol-MS-Ethanol Based [mol m ⁻² s ⁻¹]	Rate of Production of Butanol-MS-Argon Based [mol m ⁻² s ⁻¹]	Rate of Production of Butanol-GC-Based [mol m ⁻² s ⁻¹]	Rate of Production of Acetaldehyde-GC-Based [mol m ⁻² s ⁻¹]	Rate of Production of Ethene-GC-Based [mol m ⁻² s ⁻¹]
25	1.10E-8	1.03E-8	8.05E-9	2.44E-8	6.59E-9
50	9.97E-9	8.02E-9	5.23E-9	3.51E-8	7.32E-9
75	8.67E-9	4.77E-9	3.11E-9	3.40E-8	6.28E-9

(a) 3.5 mmol L⁻¹ ethanol, 0.2 g of MgO, 673 K, 1.3 atm.

Table 3: Product Distribution from Ethanol Coupling over MgO^a

Total Flow Rate [mL min ⁻¹]	Conversion of Ethanol	Selectivity of Butanol	Selectivity of Acetaldehyde	Selectivity of Ethene
25	0.23	0.34	0.52	0.14
50	0.13	0.20	0.66	0.14
75	0.07	0.13	0.73	0.13

(a) 3.5 mmol L⁻¹ ethanol, 0.2 g of MgO, 673 K, 1.3 atm.

The selectivity is a carbo- based selectivity. The following equation shows how the selectivity of butanol was calculated.

$$Selectivity_{Butanol} = \frac{2 * R_{But}}{2 * R_{Butanol} + R_{Acetaldehyde} + R_{Ethene}}$$

If the reactor were operating differentially then the conversion of ethanol would be linear with space time in the reactor. Figure 5 shows the expected differential behavior of the reactor, even for the ethanol conversion up to 23%.

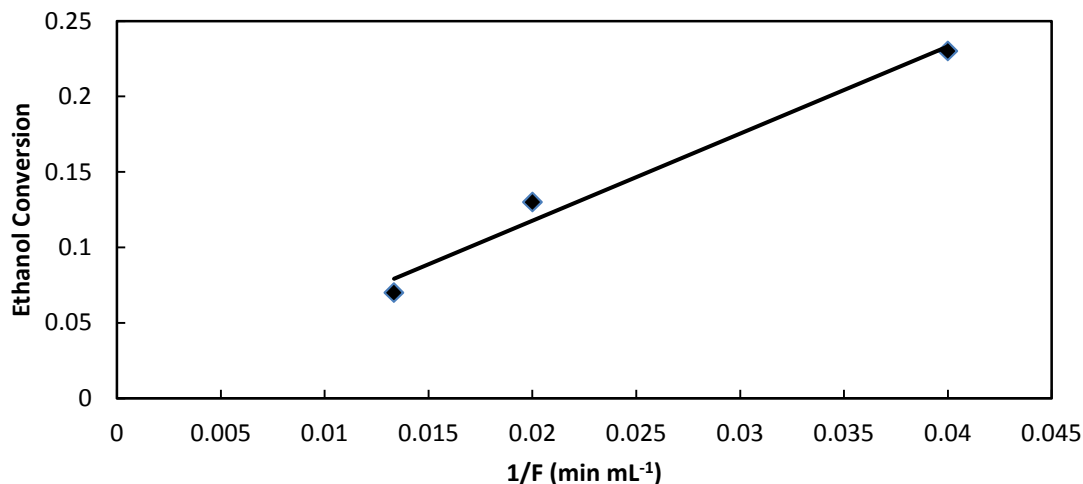


Figure 8: Relationship between the observed conversion of ethanol as a function of inverse total flow rate

The best fit line is $Ethanol\ Conversion = 5.77 \left(\frac{1}{F} \right) + 0.0023$, which gives a rate of ethanol conversion equal to approximately $5.77\ moles\ s^{-1}\ m^{-2}$ times the inverse flow rate.

Forward and reverse switches were recorded in this study, but slight pressure differences around the 4-port valve caused spikes in the data in the reverse switches (^{13}C to ^{12}C) which made the forward switch (^{13}C to ^{12}C) the one which we used to calculate parameters. The forward and reverse switch raw data can be found in the appendix. The normalized results from isotope switches performed during the reaction can be seen in Figures 9-11.

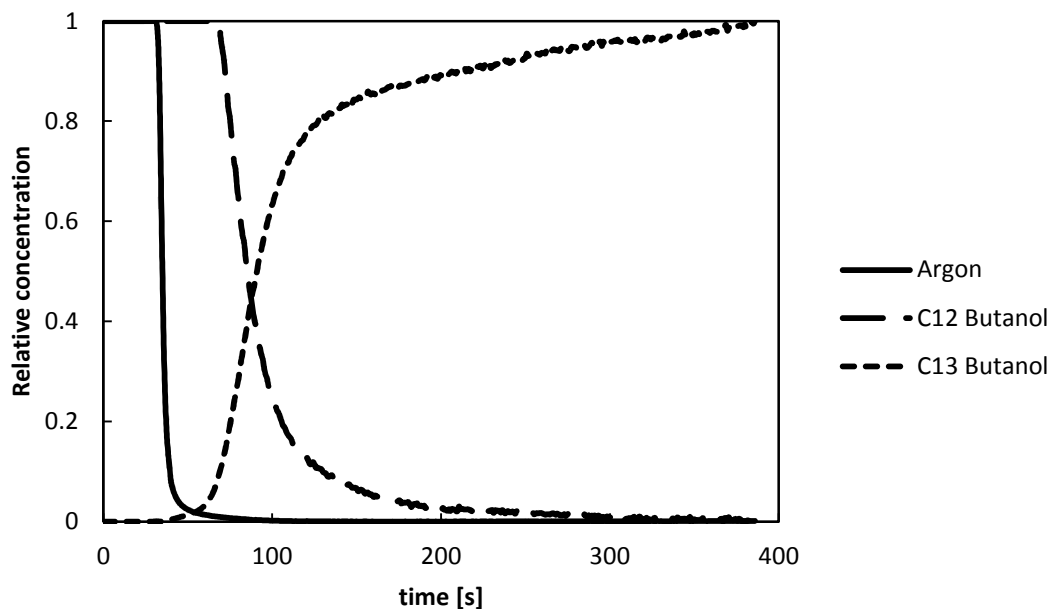


Figure 9: Isotopic transient curve for unlabeled butanol ($m/z=56$) after switching from unlabeled ethanol to ^{13}C labeled ethanol with a total flow rate of $25\text{ cm}^3\text{ min}^{-1}$ during a reaction at 3.5 mmol L^{-1} ethanol, 0.2 g of MgO , 673 K , and 1.3 atm

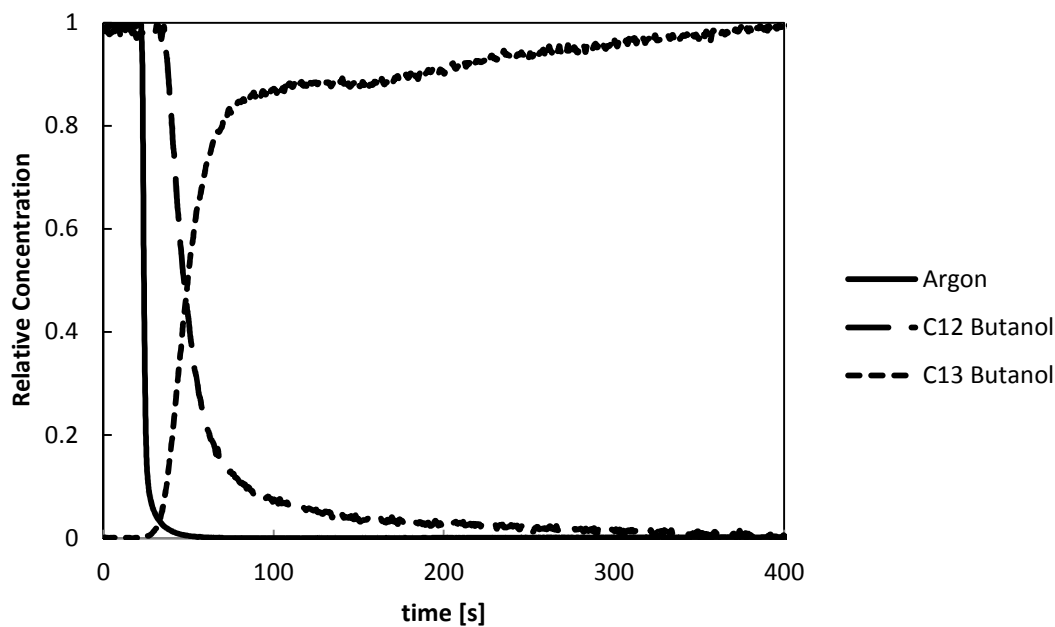


Figure 10: Isotopic transient curve for unlabeled butanol ($m/z=56$) after switching from unlabeled ethanol to ^{13}C labeled ethanol with a total flow rate of $50\text{ cm}^3\text{ min}^{-1}$ during a reaction at 3.5 mmol L^{-1} ethanol, 0.2 g of MgO , 673 K , and 1.3 atm

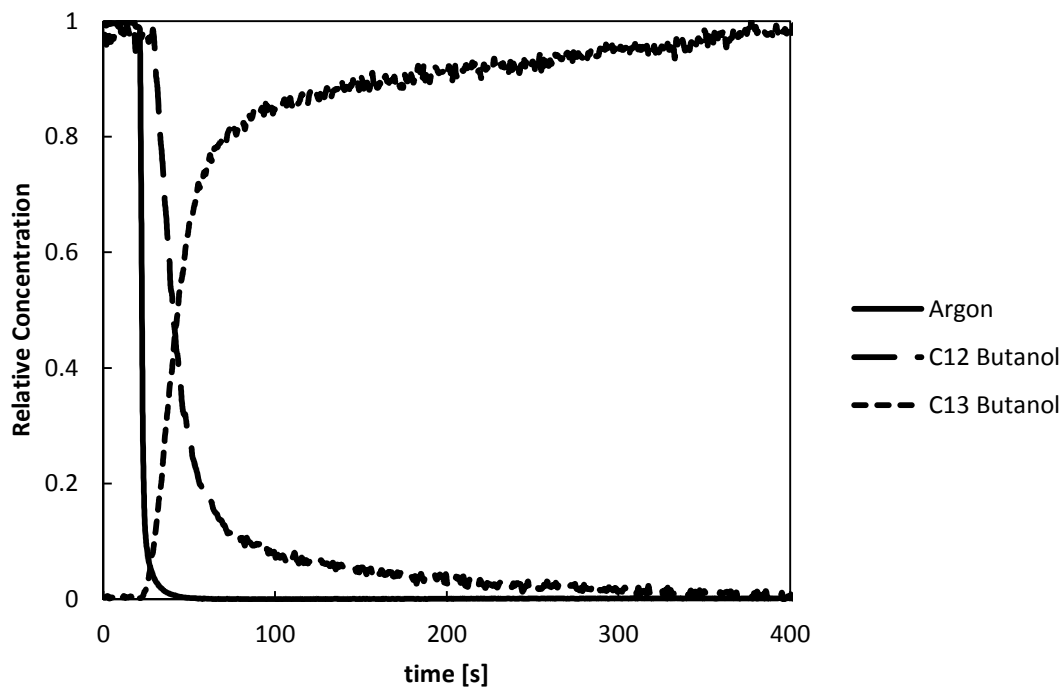


Figure 11: Isotopic transient curve for unlabeled butanol ($m/z=56$) after switching from unlabeled ethanol to ^{13}C labeled ethanol with a total flow rate of $75\text{ cm}^3\text{ min}^{-1}$ during a reaction at 3.5 mmol L^{-1} ethanol, 0.2 g of MgO , 673 K , and 1.3 atm

In order to compare the different switches, Figure 12 shows all of the ^{12}C -butanol switches (i.e. forward switches) on the same plot.

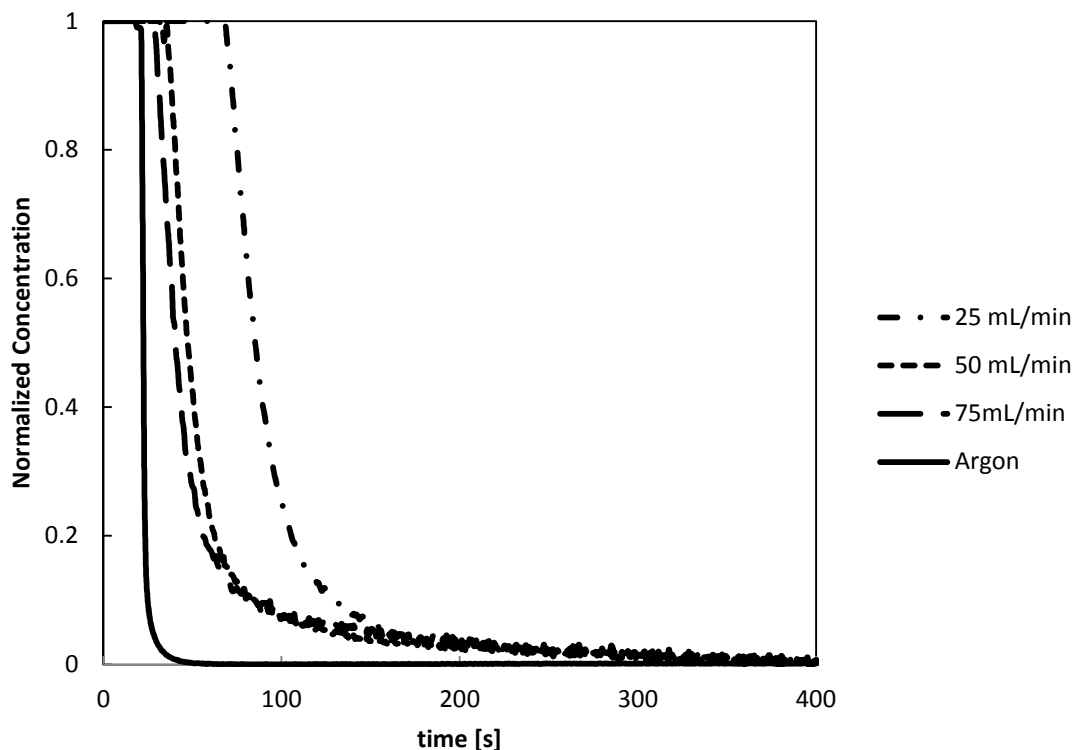


Figure 12: Isotopic transient curve for unlabeled butanol ($m/z=56$) after switching from unlabeled ethanol to ^{13}C labeled ethanol with varying total flow rates during a reaction at 3.5 mmol L^{-1} ethanol, 0.2 g of MgO , 673 K , and 1.3 atm

The mean surface residence times can be seen for the switches in table 4.

Table 4: Characteristic τ for the different flow rates.

Flow Rate [mL min^{-1}]	$1/F$ [min mL^{-1}]	τ [s]
25	0.040	60
50	0.020	36
75	0.013	32

This shows that there is product readsorption occurring on the surface of the catalyst as it exits the reactor. As expected, there is a positive correlation between the inverse of the flow rate and the mean surface residence time.

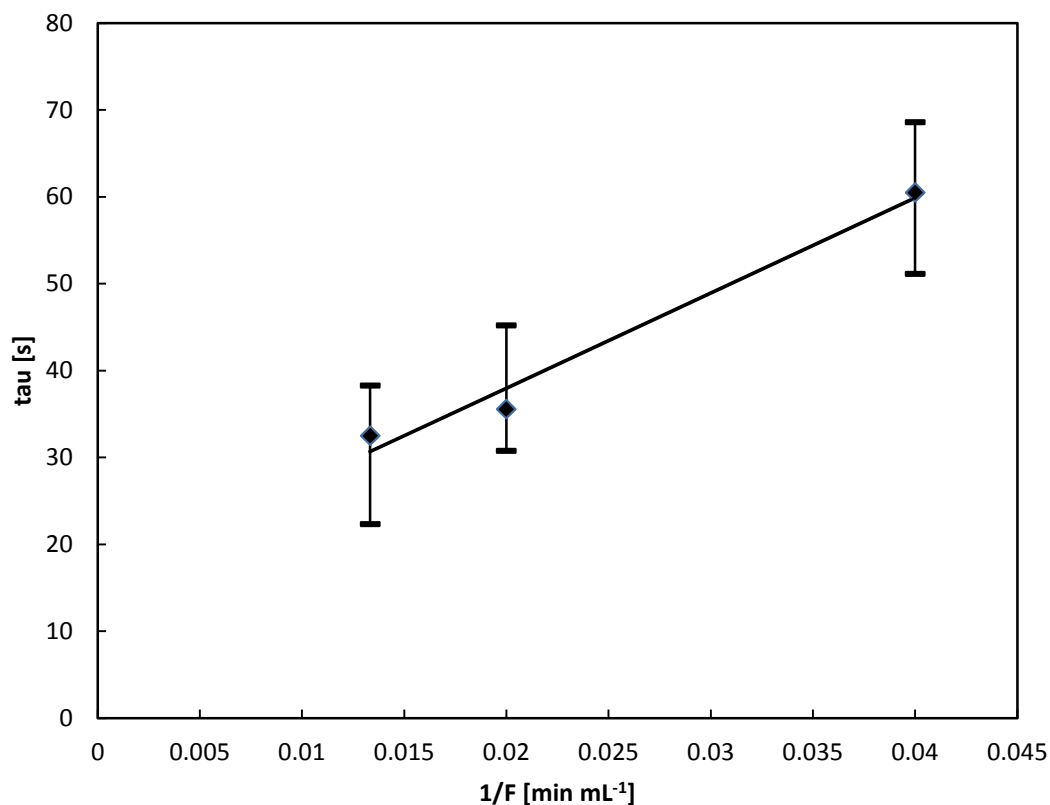


Figure 13: Relationship between the observed characteristic tau of butanol as a function of inverse total flow rate

To determine the number of surface intermediates leading to butanol, the following equation is used:

$$N_{butanol} = R_{butanol} * \tau_{butanol}$$

Where $R_{butanol}$ is the rate of production of butanol in units of $\text{mol m}^{-2} \text{s}^{-1}$ and $N_{butanol}$ is the surface coverage of intermediates in units of mol m^{-2} .

The results can be seen in Table 5.

Table 5: Calculation of the number of reactive intermediates that lead to butanol on the catalyst surface.

F [mL min ⁻¹]	Rate [mol m ⁻² s ⁻¹]	τ [s]	T.O.F. [s ⁻¹]	N _{butanol} [mol m ⁻²]
25	1.1E-8	60	0.017	6.6E-7
50	1.0E-8	36	0.028	3.6E-7
75	8.7E-9	32	0.031	2.8E-7

The coverage and residence time of the ethanol on the surface of the catalyst must also be examined. The residence time can be determined from the isotope transient after a switch in the ethanol feed. The ethanol transients for various flow rates can be found in Figures 14-16.

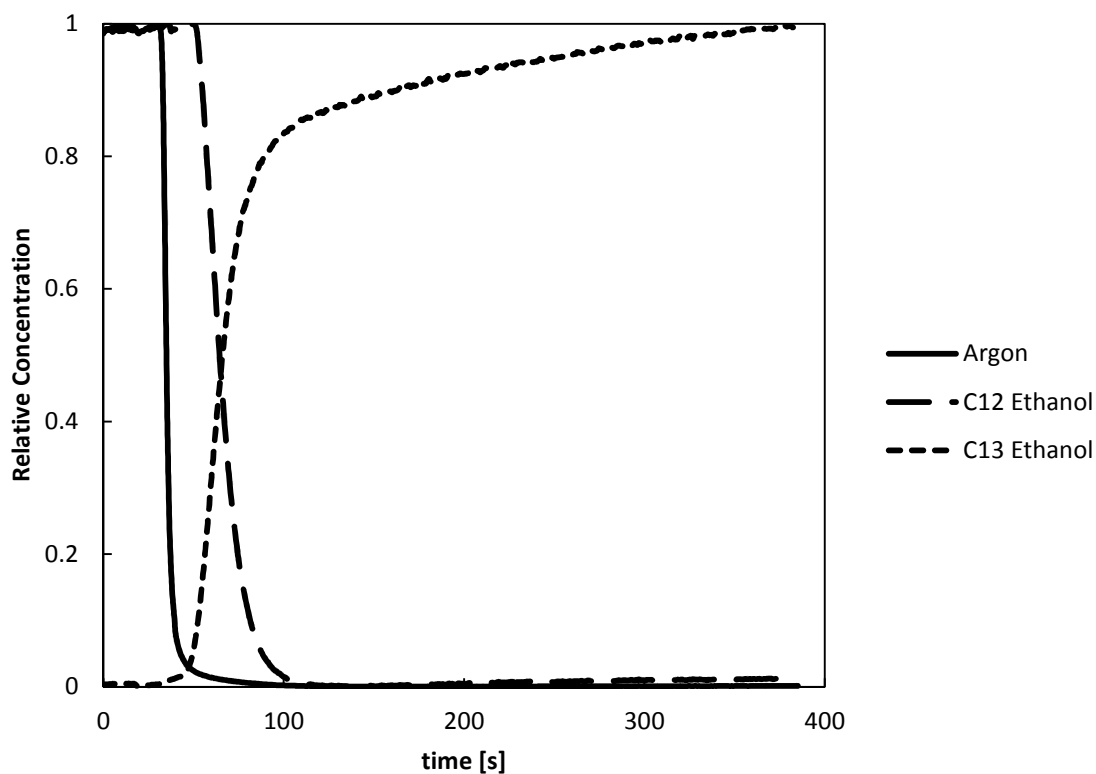


Figure 14: Isotopic transient curve for unlabeled ethanol ($m/z=31$) after switching from unlabeled ethanol to ^{13}C labeled ethanol with a total flow rate of $25 \text{ cm}^3 \text{ min}^{-1}$ during a reaction at 3.5 mmol L^{-1} ethanol, 0.2 g of MgO , 673 K , and 1.3 atm

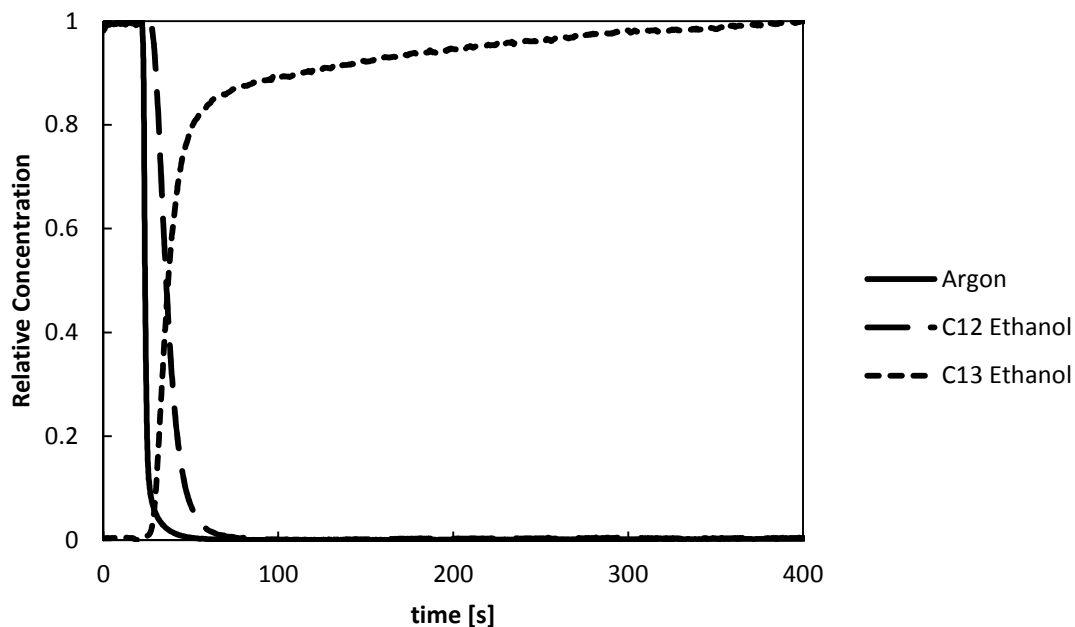


Figure 15: Isotopic transient curve for unlabeled ethanol ($m/z=31$) after switching from unlabeled ethanol to ^{13}C labeled ethanol with a total flow rate of $50\text{ cm}^3\text{ min}^{-1}$ during a reaction at 3.5 mmol L^{-1} ethanol, 0.2 g of MgO , 673 K , and 1.3 atm

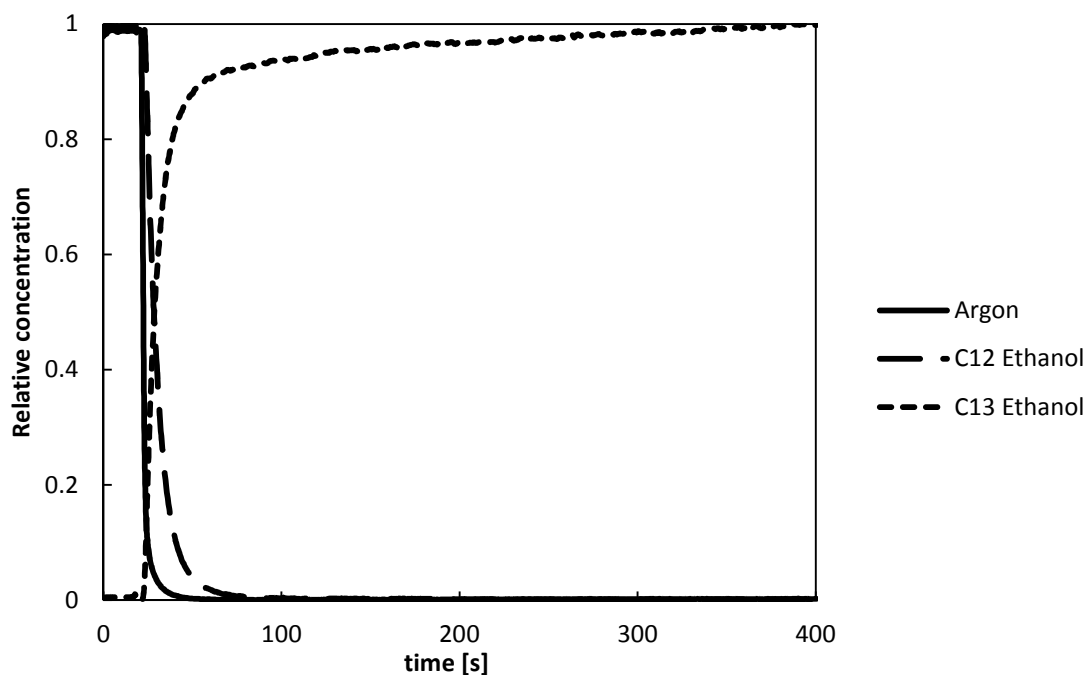
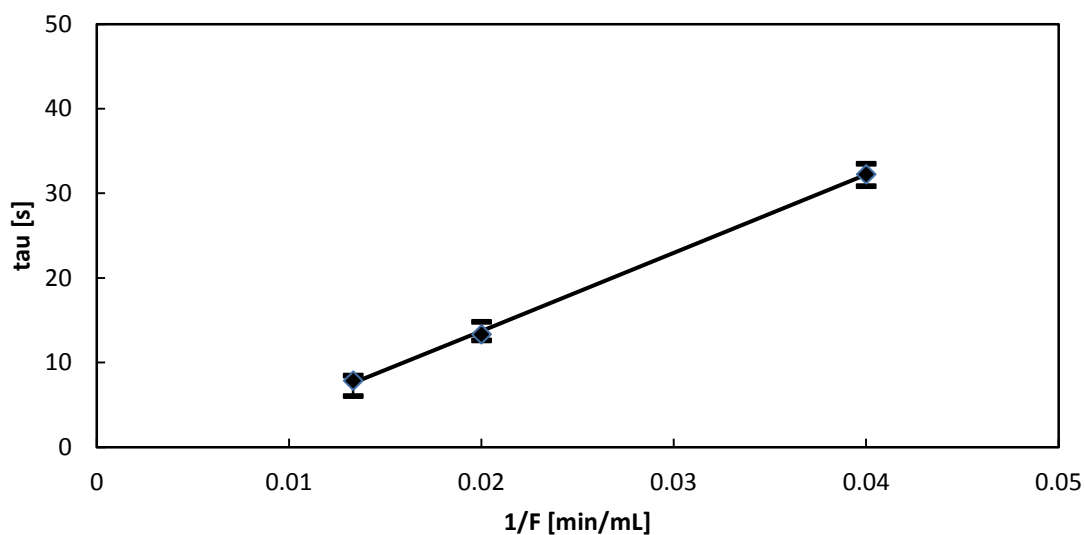


Figure 16: Isotopic transient curve for unlabeled ethanol ($m/z=31$) after switching from unlabeled ethanol to ^{13}C labeled ethanol with a total flow rate of $75\text{ cm}^3\text{ min}^{-1}$ during a reaction at 3.5 mmol L^{-1} ethanol, 0.2 g of MgO , 673 K , and 1.3 atm

Table 6: Characteristic τ for the different flow rates.

Flow Rate [mL min^{-1}]	$1/F$ [min mL^{-1}]	τ [s]
25	0.040	32
50	0.020	13
75	0.013	7.8

As with butanol, readsorption is seen on the catalyst surface.

Figure 17: Effect of Flow Rate on Characteristic τ for Ethanol

To determine the number of ethanol molecules on the surface of the catalyst at the steady state, the same method was used as before, except that the rate is now the flow rate of ethanol over the catalyst, less the amount converted.

Table 7: Calculation of the amount of ethanol on the catalyst surface.

F [mL min^{-1}]	Ethanol Flow Rate [$\text{mol m}^{-2}\text{s}^{-1}$]	τ [s]	N_{Ethanol} [mol m^{-2}]
25	$1.6\text{E-}7$	32	$5.1\text{E-}6$
50	$3.6\text{E-}7$	13	$4.7\text{E-}6$
75	$5.9\text{E-}7$	7.8	$4.6\text{E-}6$

If a suitable probe molecule is used, it is possible to determine the number of active sites on the catalyst surface. In separate experiments performed by Joseph Kozlowski using CO_2 as a probe of the MgO catalyst, he found $1.0 \mu\text{moles CO}_2 \text{ m}^{-2}$ adsorbed on the catalyst surface. Comparing this value to the number of reaction intermediates used to make butanol ($0.66 \mu\text{moles butanol m}^{-2}$ for a 25 mL min^{-1} flow rate) it would suggest that 66% of the base sites on the catalyst counted by CO_2 adsorption are being used to convert ethanol to butanol.

Based on the rock salt structure of MgO, it can be calculated from the lattice parameter that there are $9.37 \mu\text{moles m}^{-2}$ of magnesium on the (100) surface. Subsequently, it can be understood that there are also $9.37 \mu\text{moles m}^{-2}$ of oxygen atoms on the catalyst surface based on a 1:1 mole ratio in MgO. If all of the ethanol and butanol molecules on the catalyst surface are added together, it is possible to get a good approximation of how much of the catalyst surface is covered.

Table 8: Coverage of Catalyst Surface

F [mL min^{-1}]	N _{butanol} [mol m^{-2}]	N _{ethanol} [mol m^{-2}]	θ_{butanol} [$\text{mol}_{\text{but}} \text{mol}_{\text{cat}}^{-1}$]	θ_{ethanol} [$\text{mol}_{\text{eth}} \text{mol}_{\text{cat}}^{-1}$]	% of MgO Covered
25	6.6E-7	5.1E-6	0.070	0.54	61%
50	3.6E-7	4.7E-6	0.038	0.50	54%
75	2.8E-7	4.6E-6	0.030	0.49	52%

Table 8 compares the surface coverage at the various flow rates. The table shows that around 56% of the catalyst surface is covered and less than 8% of the catalyst is actively participating in the conversion of ethanol to butanol. It should be

noted that about 60% of the converted ethanol formed acetaldehyde, and another 13% formed ethene. Only a minor fraction produced butanol.

In most SSITKA studies, changing the flow rate does not change the rate of product formation since differential conversion is achieved. In our experiments, the rate of butanol production was a strong function of flow rate. It is thought that the ethanol first dehydrogenates into acetaldehyde, which leads to butanol. Indeed, Figure 15 illustrates the correlation between the acetaldehyde exit concentration and the butanol production rate. Thus, changing the flow rate will certainly change the level of acetaldehyde in the reactor, which in turn should affect the rate of butanol formation.

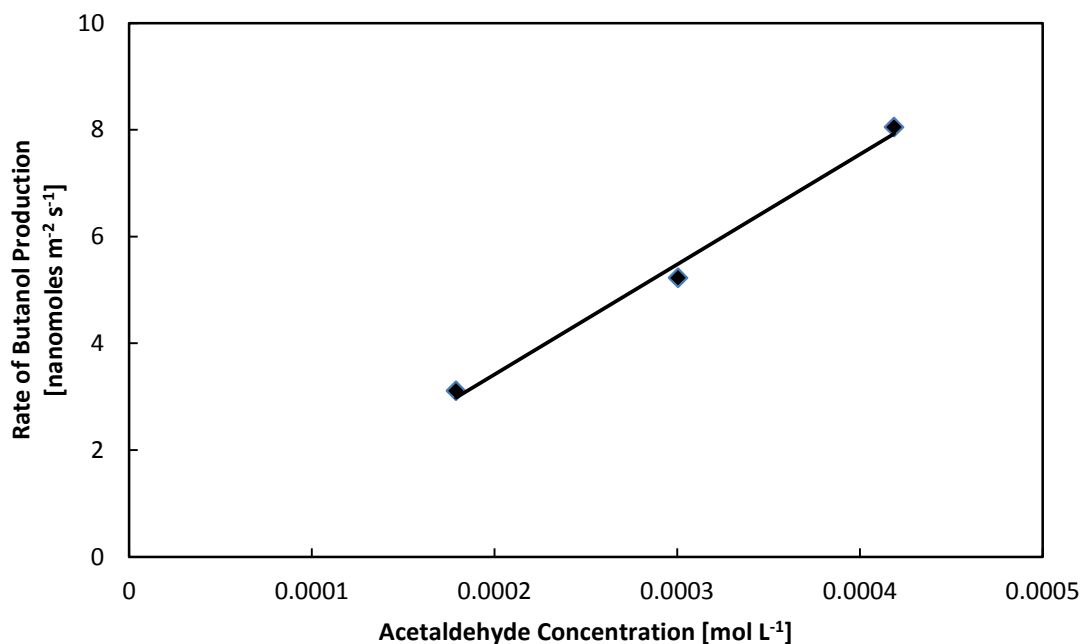


Figure 18: Relationship between the rate of butanol production as a function of the acetaldehyde concentration at the exit of the reactor.

When comparing the effect of flow rate on the characteristic tau for ethanol and the effect of flow rate on the characteristic tau for butanol an interesting observation can be noted.

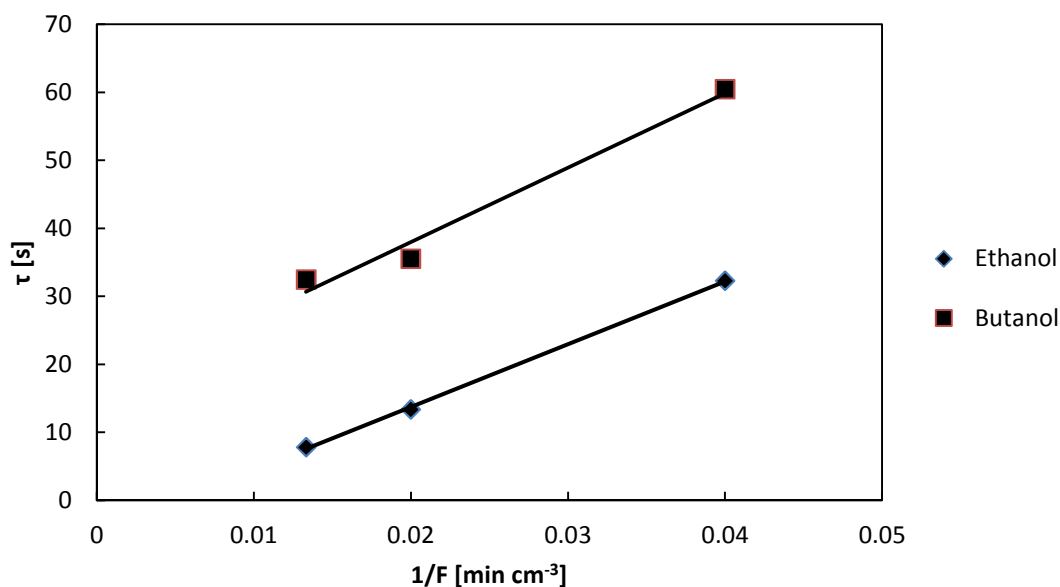


Figure 19: Comparing the Effect of Flow Rate on the Characteristic tau for Ethanol and Butanol

The slopes of the lines are similar. The differences in the ethanol and butanol values are therefore similar at each flow rate. Evidently the readsorption of ethanol is similar to that of butanol on the MgO. Taking the average of the differences from ethanol and butanol gives us a characteristic tau for butanol production of 25 seconds.

When running control experiments, a small holdup of ethanol within the system was found. The system was pre-treated as if there was a catalyst within the system, but no catalyst was present. The results of the control experiments can be seen in Figures 20-22.

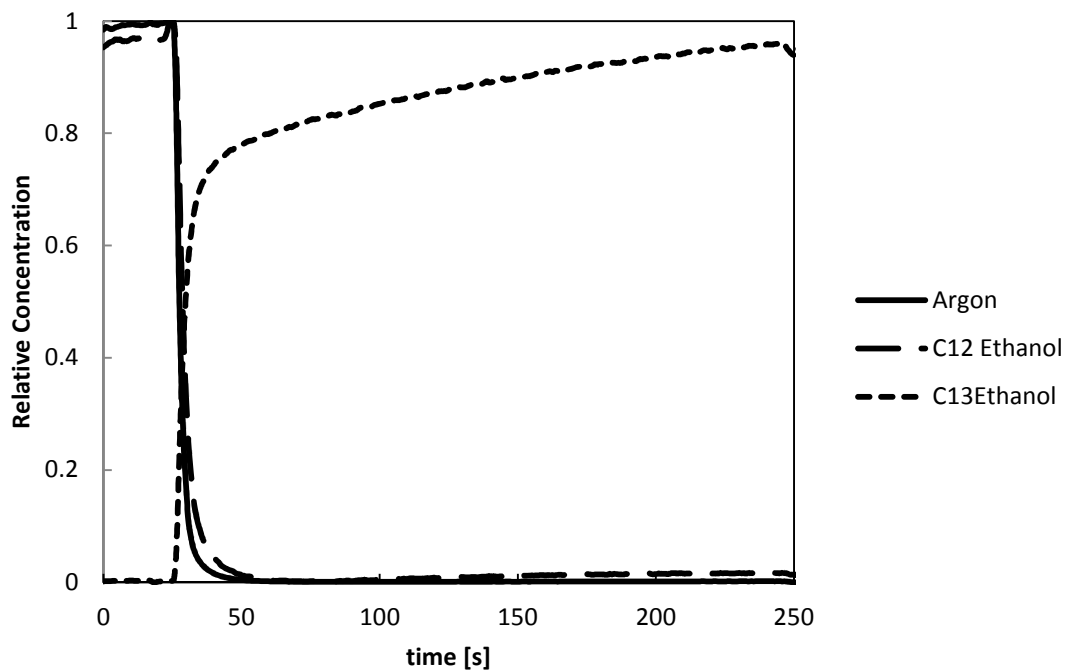


Figure 20: Analysis of ethanol in an empty reactor switch at 25 mL min⁻¹

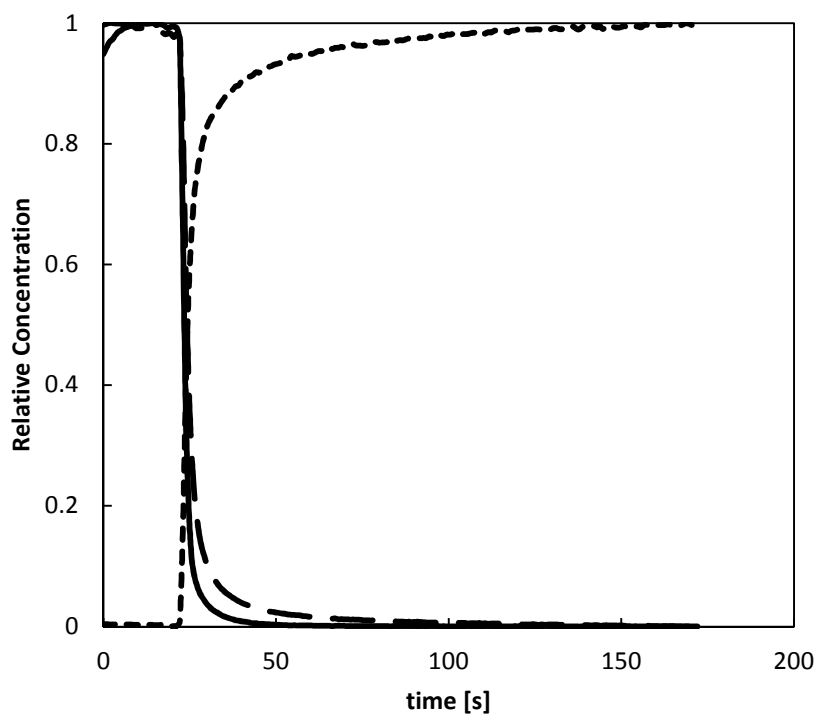


Figure 21: Analysis of ethanol in an empty reactor switch at 50 mL min⁻¹

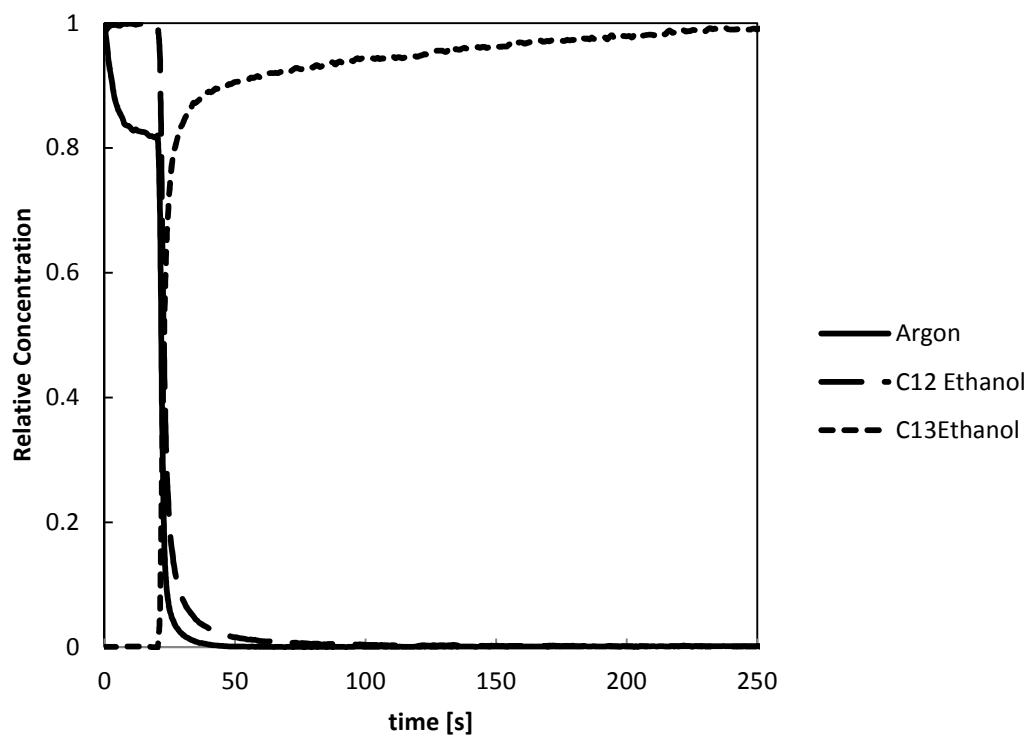


Figure 22: Analysis of ethanol in an empty reactor switch at 75 mL min^{-1}

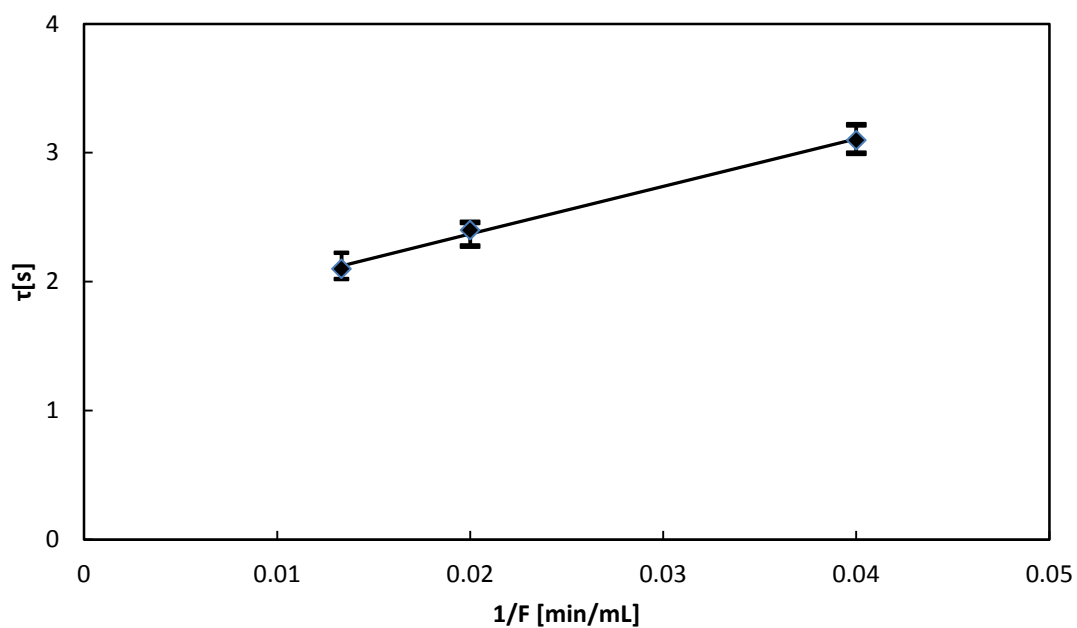


Figure 23: Effect of flow rate on space time of ethanol.

These results show that something within the system is causing a small hold-up for the ethanol. Other blank reactor experiments were ran at a total flow rate of 50 mL min⁻¹ and 673 K and examined to check the reaction rate of the reactor. The average conversion of ethanol in these experiments is about 5% and all of it is converted into acetaldehyde.

The error bars were calculated using the methods described in “Error Analysis of Experiments, A Manual for Engineering Students.” The error is based off of how accurate the best fit line is to a given set of data points. Using the given data, and a best fit line, it is possible to calculate S_x , S_y , and S_{xx} using the following equations.

$$S_x = \left[\frac{1}{n-1} \sum_{i=1}^n (x_i - \bar{x})^2 \right]$$

$$S_y = \left[\frac{1}{n-2} \sum_{i=1}^n (y_i - \hat{y}_i)^2 \right]$$

$$S_{xx} = \sum_{i=1}^n x_i^2 - \left(\frac{1}{n} \right) \left(\sum_{i=1}^n x_i \right)^2$$

Where \bar{x} is the average value of x, and \hat{y} is the calculated value of y based on the best fit line. Using these values it is possible to calculate a 95% prediction interval around the best fit line by solving for P_y using the following equation:

$$P_y = 2 \left\{ S_y^2 \left[1 + \frac{1}{n} + \frac{(x - \bar{x})^2}{S_{xx}} \right] \right\}^2$$

Chapter 6: Conclusions

Ethanol coupling over MgO is a multistep reaction, with ethanol being converted into acetaldehyde, which in turn is converted into butanol. This causes the rate of ethanol conversion to change when the flow rate is changed, which leads to a change in the rate of butanol production. Within the flow rates studied, the rate of production of butanol varied from 3 to 8 nanomoles $\text{m}^{-2} \text{s}^{-1}$. The major product in all three flow rates examined was acetaldehyde, with ethene consisting of 14% of the product in all conditions as well.

The coverage of reactive intermediates leading to butanol on MgO was 66% based on separate CO_2 adsorption measurements of the base site density. However, based on the number of exposed MgO atom pairs, less than 8% of the catalyst is covered with reaction intermediates, while about 51% of the surface of the catalyst is covered with absorbed ethanol, presumably as ethoxide.

The mean surface residence time of the intermediates in the ethanol coupling reaction leading to butanol is 25 seconds. A new method was used to solve for this due to variation of acetaldehyde concentration with changing flow rate. The value was solved by noticing the difference between the characteristic tau of butanol and the characteristic tau of ethanol was consistent over the various flow rates. It would be important to be able to separate the reaction of ethanol being converted into acetaldehyde, and acetaldehyde being converted into butanol.

A potential next step of this project would be to study the reaction of acetaldehyde and hydrogen gas being converted into butanol. With the second part of

the reaction in our current study being looked at, we could find out more details about the mechanism. If the mean surface residence time of the reaction was low, it would help support our hypothesis that the dehydrogenation of the ethanol is the rate limiting step in the mechanism.

Appendix

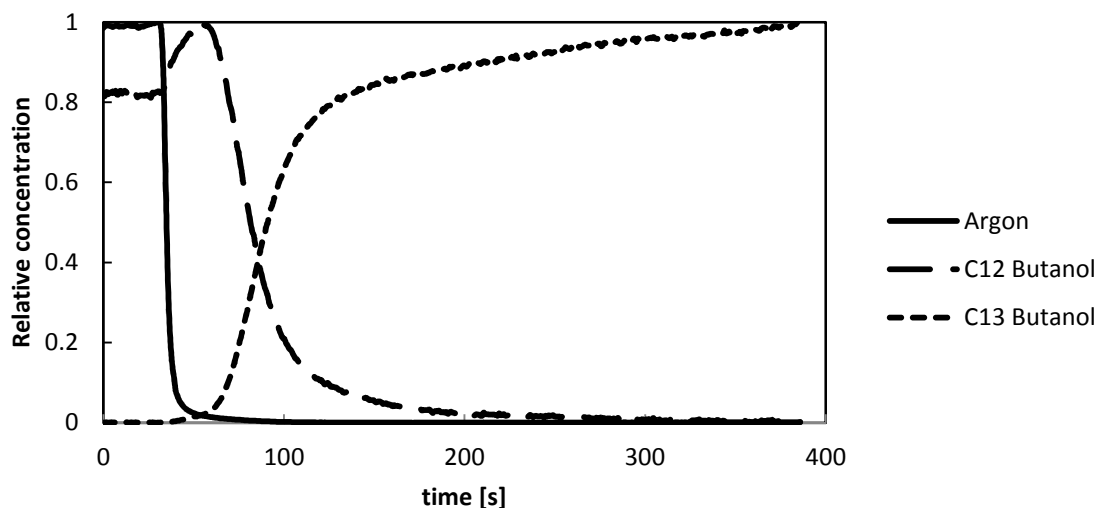


Figure 24: Isotopic transient curve for unlabeled butanol ($m/z=56$) after switching from unlabeled ethanol to ^{13}C labeled ethanol with a total flow rate of $25\text{ cm}^3\text{ min}^{-1}$ during a reaction at 3.5 mmol L^{-1} ethanol, 0.2 g of MgO , 673 K , and 1.3 atm . Raw data normalized.

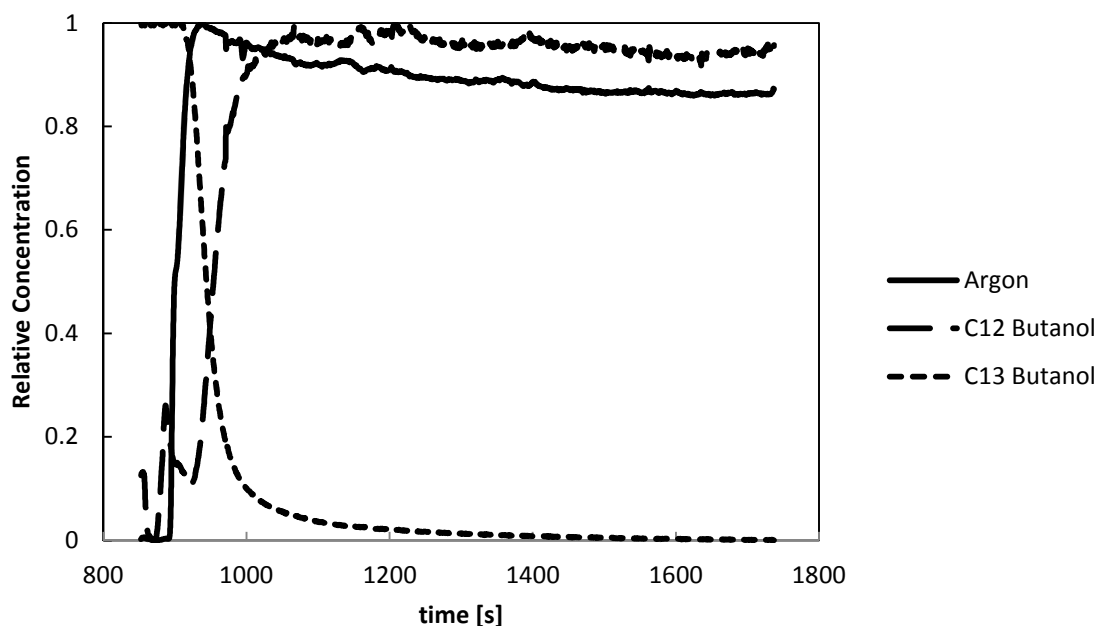


Figure 25: Isotopic transient curve for unlabeled butanol ($m/z=56$) after switching from ^{13}C labeled ethanol to unlabeled ethanol with a total flow rate of $25\text{ cm}^3\text{ min}^{-1}$ during a reaction at 3.5 mmol L^{-1} ethanol, 0.2 g of MgO , 673 K , and 1.3 atm . Raw data normalized.

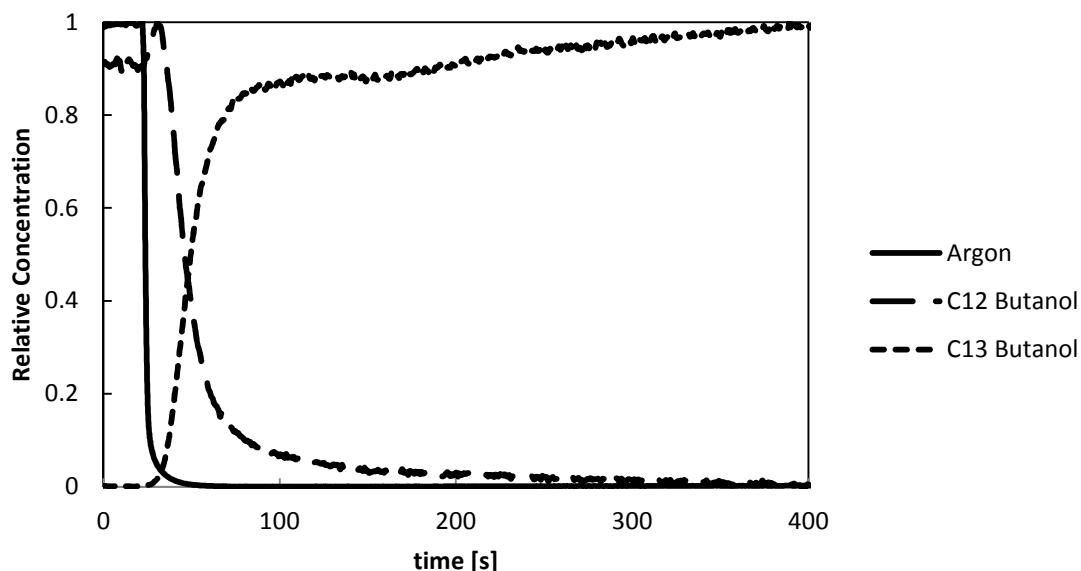


Figure 26: Isotopic transient curve for unlabeled butanol ($m/z=56$) after switching from unlabeled ethanol to ^{13}C labeled ethanol with a total flow rate of $50 \text{ cm}^3 \text{ min}^{-1}$ during a reaction at 3.5 mmol L^{-1} ethanol, 0.2 g of MgO , 673 K , and 1.3 atm . Raw data normalized.

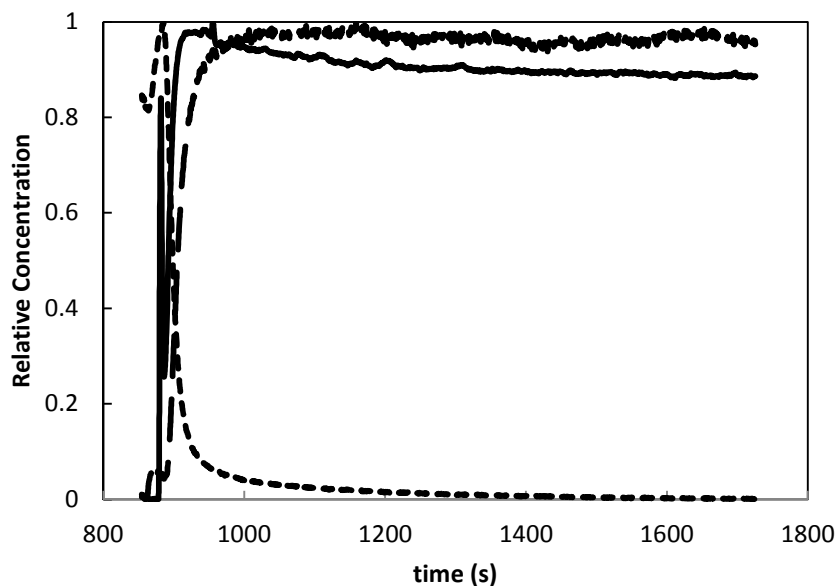


Figure 27: Isotopic transient curve for unlabeled butanol ($m/z=56$) after switching from ^{13}C labeled ethanol to unlabeled ethanol with a total flow rate of $50 \text{ cm}^3 \text{ min}^{-1}$ during a reaction at 3.5 mmol L^{-1} ethanol, 0.2 g of MgO , 673 K , and 1.3 atm . Raw data normalized.

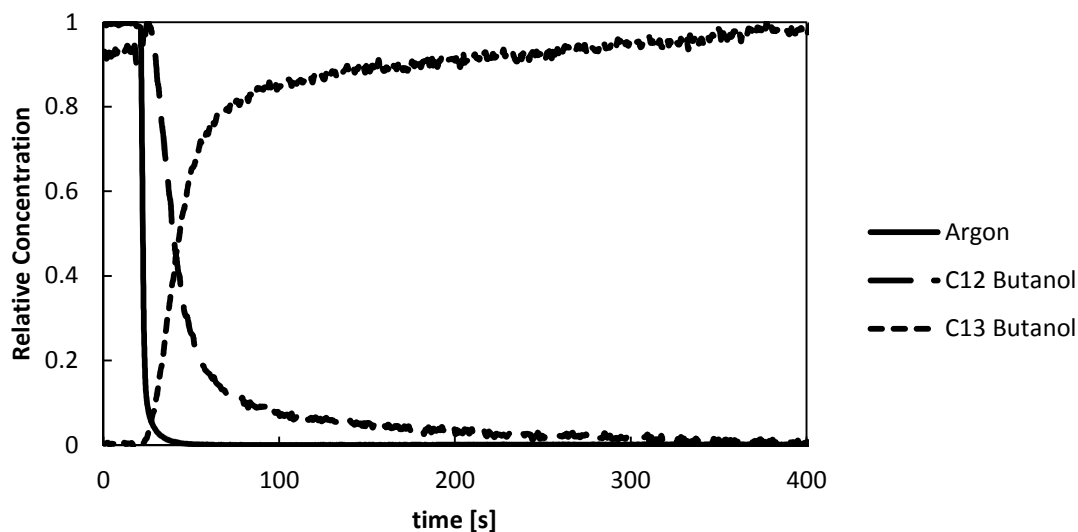


Figure 28: Isotopic transient curve for unlabeled butanol ($m/z=56$) after switching from unlabeled ethanol to ^{13}C labeled ethanol with a total flow rate of $75\text{ cm}^3\text{ min}^{-1}$ during a reaction at 3.5 mmol L^{-1} ethanol, 0.2 g of MgO , 673 K , and 1.3 atm . Raw data normalized.

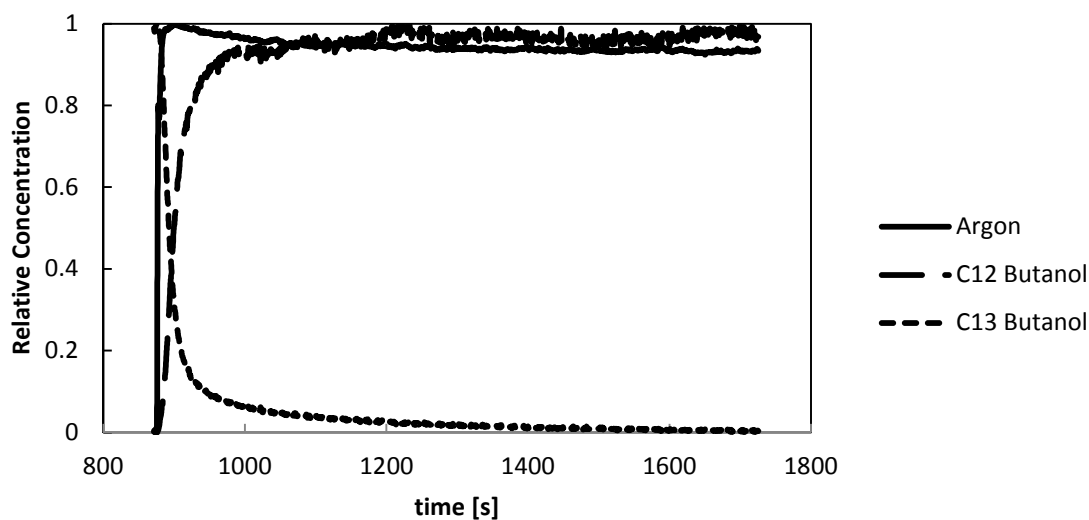


Figure 29: Isotopic transient curve for unlabeled butanol ($m/z=56$) after switching from ^{13}C labeled ethanol to unlabeled ethanol with a total flow rate of $75\text{ cm}^3\text{ min}^{-1}$ during a reaction at 3.5 mmol L^{-1} ethanol, 0.2 g of MgO , 673 K , and 1.3 atm . Raw data normalized.

Table 9: Characteristic tau of butanol and ethanol

Total flow rate (mL/min)	Forward or Reverse switch	¹² C-butanol	¹³ C-butanol	¹² C-ethanol	¹³ C-ethanol
25	Forward	60*	79	32*	52
25	Reverse	94	59	21	28
50	Forward	36*	51	13*	34
50	Reverse	45	20	1.9	6.9
75	Forward	32*	52	7.8*	20
75	Reverse	60	40	6.2	10

*Values were used in the study.

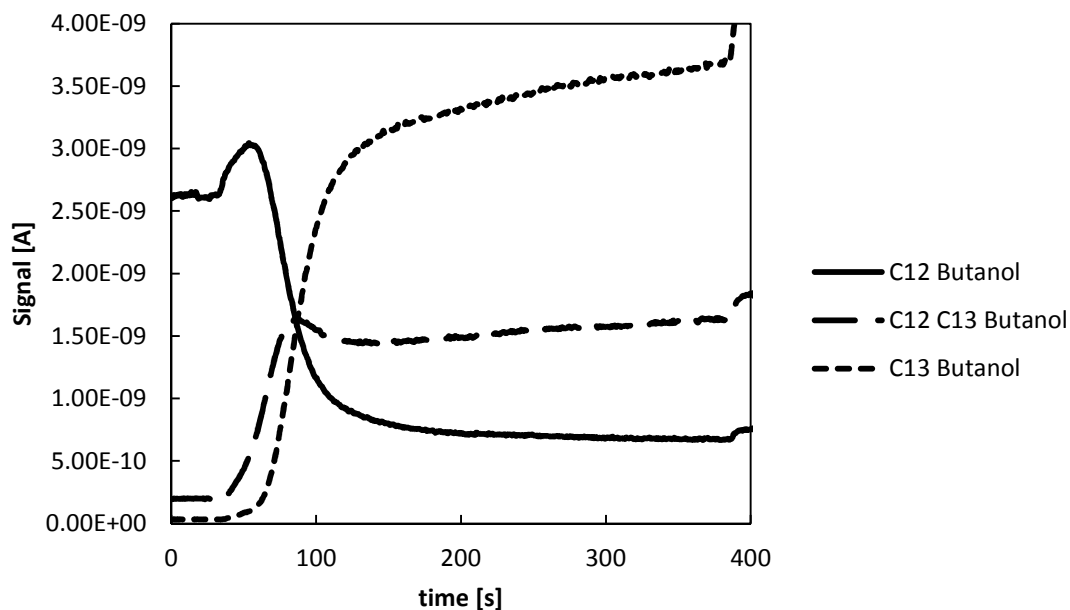


Figure 30: Isotopic transient curve for unlabeled butanol ($m/z=56$), ^{12}C - ^{13}C -butanol ($m/z=58$), and ^{13}C -butanol ($m/z=60$) after switching from unlabeled ethanol to ^{13}C labeled ethanol with a total flow rate of $25\text{ cm}^3\text{ min}^{-1}$ during a reaction at 3.5 mmol L^{-1} ethanol, 0.2 g of MgO , 673 K , and 1.3 atm . Raw data.

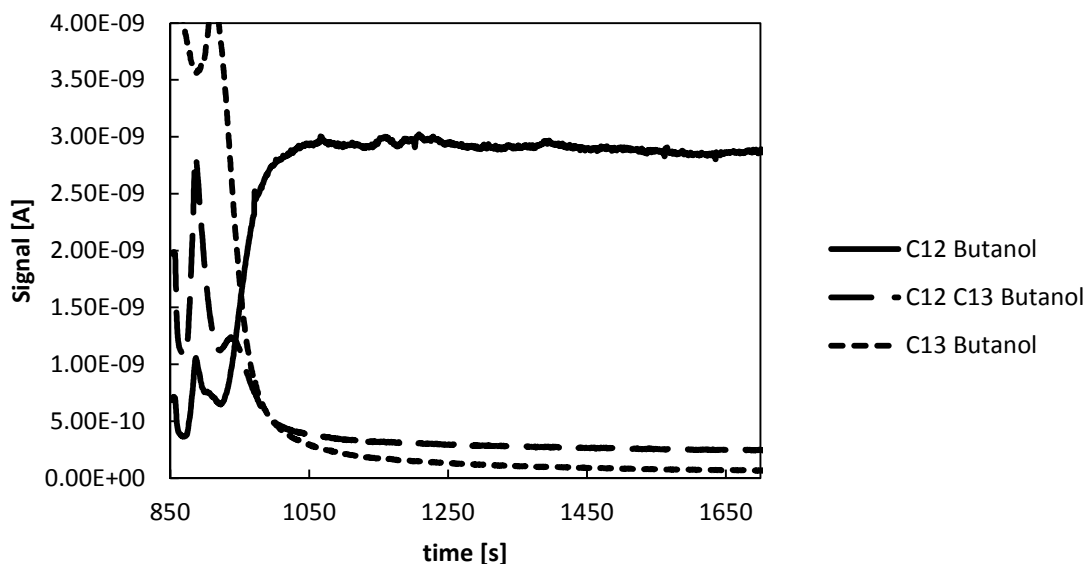


Figure 31: Isotopic transient curve for unlabeled butanol ($m/z=56$), ^{12}C - ^{13}C -butanol ($m/z=58$), and ^{13}C -butanol ($m/z=60$) after switching from ^{13}C labeled ethanol to unlabeled ethanol with a total flow rate of $25\text{ cm}^3\text{ min}^{-1}$ during a reaction at 3.5 mmol L^{-1} ethanol, 0.2 g of MgO , 673 K , and 1.3 atm . Raw data.

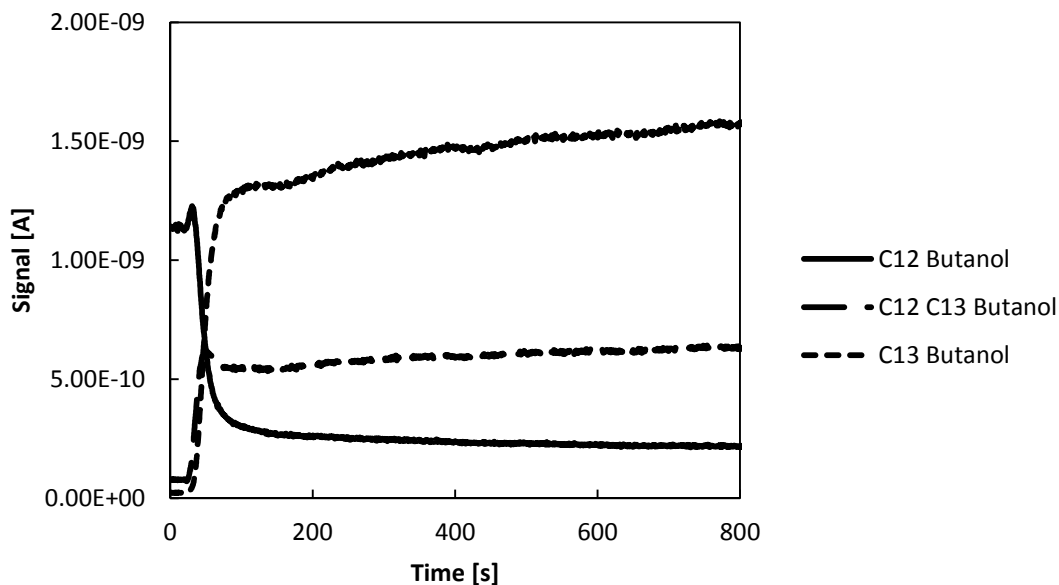


Figure 32: Isotopic transient curve for unlabeled butanol ($m/z=56$), ^{12}C - ^{13}C -butanol ($m/z=58$), and ^{13}C -butanol ($m/z=60$) after switching from unlabeled ethanol to ^{13}C labeled ethanol with a total flow rate of $50\text{ cm}^3\text{ min}^{-1}$ during a reaction at 3.5 mmol L^{-1} ethanol, 0.2 g of MgO , 673 K , and 1.3 atm . Raw data.

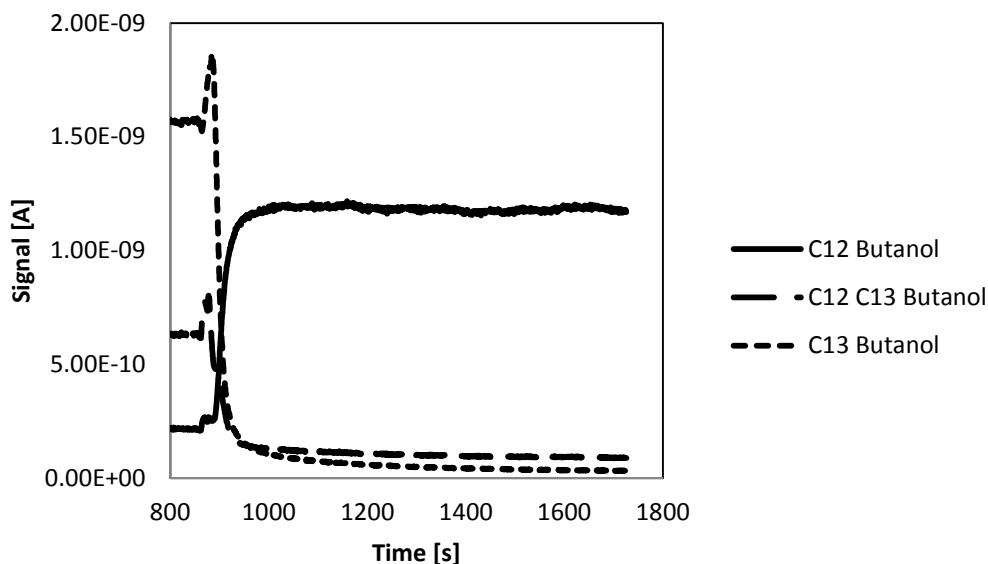


Figure 33: Isotopic transient curve for unlabeled butanol ($m/z=56$), ^{12}C - ^{13}C -butanol ($m/z=58$), and ^{13}C -butanol ($m/z=60$) after switching from ^{13}C labeled ethanol to unlabeled ethanol with a total flow rate of $50\text{ cm}^3\text{ min}^{-1}$ during a reaction at 3.5 mmol L^{-1} ethanol, 0.2 g of MgO , 673 K , and 1.3 atm . Raw data.

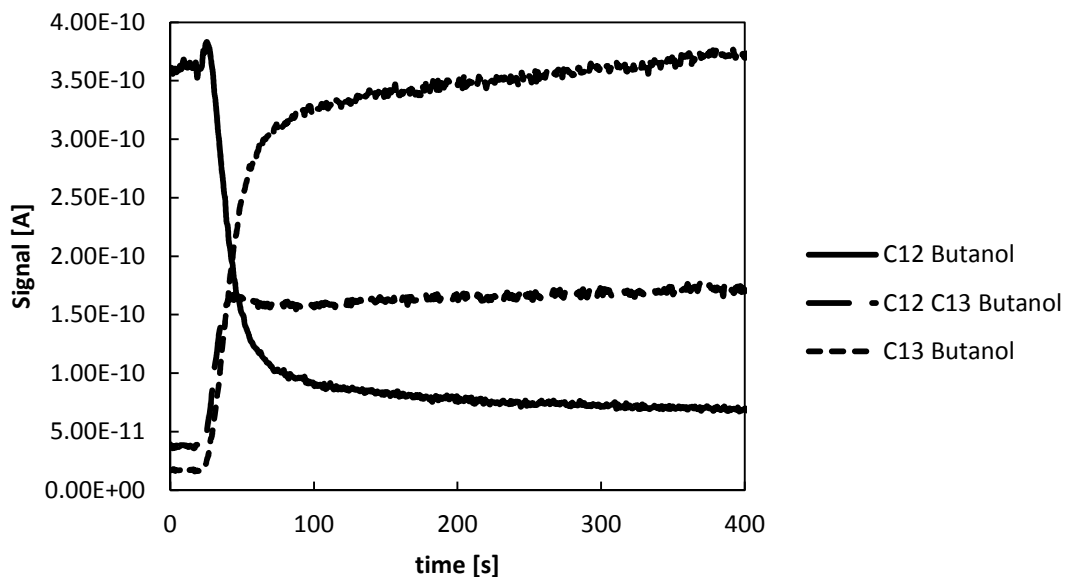


Figure 34: Isotopic transient curve for unlabeled butanol ($m/z=56$), ^{12}C - ^{13}C -butanol ($m/z=58$), and ^{13}C -butanol ($m/z=60$) after switching from unlabeled ethanol to ^{13}C labeled ethanol with a total flow rate of $75\text{ cm}^3\text{ min}^{-1}$ during a reaction at 3.5 mmol L^{-1} ethanol, 0.2 g of MgO , 673 K , and 1.3 atm . Raw data.

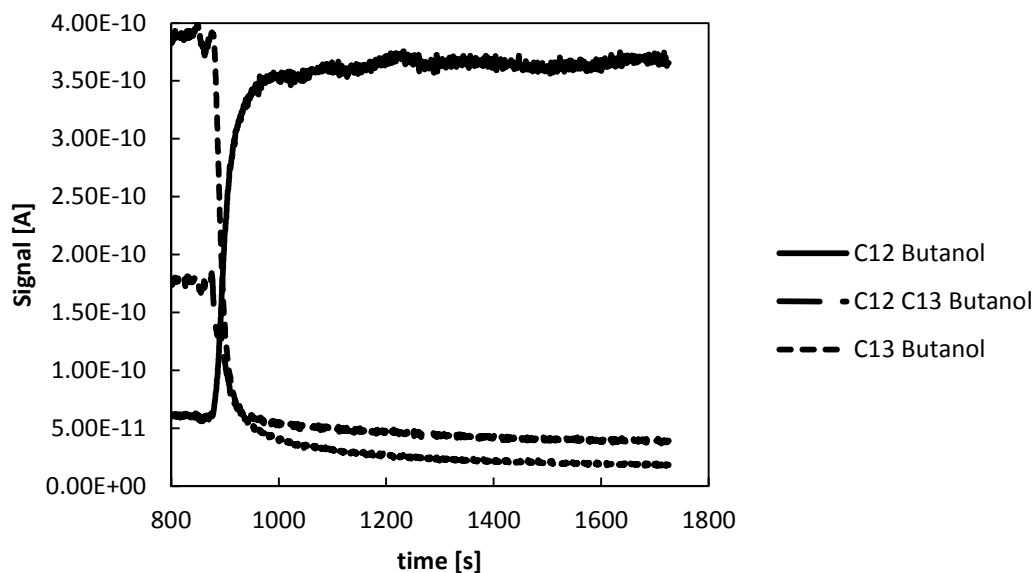


Figure 35: Isotopic transient curve for unlabeled butanol ($m/z=56$), ^{12}C - ^{13}C -butanol ($m/z=58$), and ^{13}C -butanol ($m/z=60$) after switching from ^{13}C labeled ethanol to unlabeled ethanol with a total flow rate of $75\text{ cm}^3\text{ min}^{-1}$ during a reaction at 3.5 mmol L^{-1} ethanol, 0.2 g of MgO , 673 K , and 1.3 atm . Raw data.

References

1. *Butanol*, SIDS Initial Assessment Report, Geneva: United Nations Environment Programme, April 2005, <http://www.inchem.org/documents/sids/sids/71363.pdf>.
2. Ezeji, Thaddeus C. "Biobutanol production by solventogenic *Clostridium* species: recent progress and challenges ahead."
http://bioenergy.illinois.edu/education/12seminars/02_ezeji.pdf
3. James Jacobs, Ag Economist. "Ethanol from Sugar". United States Department of Agriculture. <http://www.rurdev.usda.gov/rbs/pub/sep06/ethanol.htm>.
4. Renewable Fuels Association. "Statistics, Historic U.S. Fuel Ethanol Production"
<http://www.ethanolrfa.org/pages/statistics#A>
5. Marcel Guerbet (1909). "Condensation de l'alcool isopropylique avec son derive sode; formation du methylisobutylcarbinol et du dimethyl-2.4-heptanol-6". *Comptes rendus de l'Académie des sciences* 149: 129–132.
<http://gallica.bnf.fr/ark:/12148/bpt6k3103r/f129.table>.
6. O'Lenick, Jr., Anthony J. "A Review of Guerbet Chemistry"
http://www.zenitech.com/documents/guerbet_chemistry.pdf
7. Veibel, S, and Ji Nielsen. "ON THE MECHANISM OF THE GUEXBET REACTION."
Tetrahedron 23.4 (1967) : 1723–1733
8. Matsu-Ura, Toyomi et al. "Guerbet reaction of primary alcohols leading to beta-alkylated dimer alcohols catalyzed by iridium complexes." *The Journal of Organic Chemistry* 71.21 (2006) : 8306-8308.

9. Carlini, C. "Selective synthesis of isobutanol by means of the Guerbet reaction Part 1. Methanol/n-propanol condensation by using copper based catalytic systems." *Journal of Molecular Catalysis A: Chemical* 184 (2002) 273–280
10. Carlini, C. "Selective synthesis of isobutanol by means of the Guerbet reaction Part 2. Reaction of methanol/ethanol and methanol/ethanol/n-propanol mixtures over copper based/MeONa catalytic systems." *Journal of Molecular Catalysis A: Chemical* 200.1-2 (2003) : 137-146.
11. Carlini, C. "Selective synthesis of isobutanol by means of the Guerbet reaction Part 3: Methanol/n-propanol condensation by using bifunctional catalytic systems based on nickel, rhodium and ruthenium species with basic components." *Journal of Molecular Catalysis A: Chemical* 206.1-2 (2003) : 409-418.
12. Carlini, Carlo et al. "Guerbet condensation of methanol with n-propanol to isobutyl alcohol over heterogeneous bifunctional catalysts based on Mg–Al mixed oxides partially substituted by different metal components." *Journal of Molecular Catalysis A: Chemical* 232.1-2 (2005) : 13-20.
13. P. Biloen "Transient Kinetic Methods," *J. Mol. Cata.* 21, 17 (1983)
14. S. L. Shannon and J. G. Goodwin "Characterization of Catalytic Surfaces by Isotopic-Transient Kinetics during Steady-State Reaction," *Chem. Rev.* 95 (1995) (3), 677-695.
15. Ocal, Meltem et al. "Steady State Isotopic Transient Kinetic Analysis (SSITKA) Investigation of NO Reduction with CO over Perovskite Catalysts." *Industrial & Engineering Chemistry Research* 33.12 (1994) : 2930-2934.

16. Papavasiliou, J, G Avgouropoulos, and T Ioannides. "Steady-state isotopic transient kinetic analysis of steam reforming of methanol over Cu-based catalysts." *Applied Catalysis B Environmental* 88.3-4 (2009) : 490-496.
17. Van Dijk, H A J, J H B J Hoebink, and J C Schouten. "Steady-state isotopic transient kinetic analysis of the Fischer–Tropsch synthesis reaction over cobalt-based catalysts." *Chemical Engineering Science* 56.4 (2001) : 1211-1219.
18. Bal'zhinimaev, B S, E M Sadovskaya, and A P Suknev. "Transient isotopic kinetics study to investigate reaction mechanisms." *Chemical Engineering Journal* 154.1-3 (2009) : 2-8.
19. Diez, V.K., Apesteguia, J.I., Cosimo, D. "Aldol condensation of citral with acetone on MgO and alkali-promoted MgO catalysts" *Journal of Catalysis*. 240.2. (2006) 235-244
20. Zhang, G., Hattori, H., Kozo, T. "Aldol condensation of acetone/acetone d₆ over magnesium oxide and lanthanum oxide" *Applied Catalysis*. 40. (1988) 183-190
21. Shen, W., Tompsett, G.A., et al. "Liquid phase aldol condensation reactions with MgO–ZrO₂ and shape-selective nitrogen-substituted NaY" *Applied Catalysis A: General*. 392.1-2 (2011) 57-68
22. Ndou, A. "Dimerisation of ethanol to butanol over solid-base catalysts." *Applied Catalysis A: General* 251.2 (2003) : 337-345.
23. Soc, J Chem et al. "A Low-pressure Guerbet Reaction over Magnesium Oxide Catalyst." *Synthesis* (1990) : 1558-1559. Print.

24. Varisli, D, T Dogu, and G Dogu. "Ethylene and diethyl-ether production by dehydration reaction of ethanol over different heteropolyacid catalysts." *Chemical Engineering Science* 62.18-20 (2007) : 5349-5352.
25. National Institute of Standards and Technology, NIST Chemistry WebBook
<http://webbook.nist.gov/chemistry/>
26. "Mass Spectrometer" <http://www.pfeiffer-vacuum.com/products/mass-spectrometer/container.action>